CCL28 modulates neutrophil responses during infection with mucosal pathogens

Araceli Perez-Lopez[1,2,3], Steven Silva[1], Michael H. Lee[1], Nicholas Dillon[1], Stephanie L. Brandt[1], Romana R. Gerner[1], Karine Melchior[1,4], Gregory T. Walker[1], Victor A. Sosa-Hernandez[5,6], Rodrigo Cervantes-Diaz[5,6], Sandra Romero-Ramirez[5,7], Jose L. Maravillas-Montero[5], Sean-Paul Nuccio[1,2], Victor Nizet[1,8,9], and Manuela Raffatellu[1,2,9,10*]

[1] Division of Host-Microbe Systems & Therapeutics, Department of Pediatrics, University of California San Diego, La Jolla, CA 92093, USA

[2] Department of Microbiology and Molecular Genetics, University of California Irvine, Irvine, CA 92697, USA

[3] Biomedicine Research Unit, Facultad de Estudios Superiores Iztacala, Universidad Nacional Autónoma de México. Tlalnepantla, State of México 54090, México.

[4] School of Pharmaceutical Sciences, São Paulo State University (UNESP), Araraquara, São Paulo, Brazil

[5] Red de Apoyo a la Investigación, Universidad Nacional Autónoma de México and Instituto Nacional de Ciencias Médicas y Nutrición Salvador Zubirán, México City 14080, México

[6] Departamento de Biomedicina Molecular, Centro de Investigación y de Estudios Avanzados del Instituto Politécnico Nacional, Mexico City 07360, México

[7] Facultad de Medicina, Universidad Nacional Autónoma de México, Mexico City 04510, México

[8] Skaggs School of Pharmacy and Pharmaceutical Sciences, University of California San Diego, La Jolla, CA, 92093, USA

[9] Center for Microbiome Innovation, University of California San Diego, La Jolla, CA 92093, USA

[10] Chiba University-UC San Diego Center for Mucosal Immunology, Allergy, and Vaccines (CU-UCSD cMAV), La Jolla, CA 92093, USA

*To whom correspondence should be addressed:
Manuela Raffatellu - Email: manuelar@ucsd.edu

Abstract

The chemokine CCL28 is highly expressed in mucosal tissues, but its role during infection is not well understood. Here we show that CCL28 promotes neutrophil accumulation to the gut of mice infected with *Salmonella* and to the lung of mice infected with *Acinetobacter*. Neutrophils isolated from the infected mucosa expressed the CCL28 receptors CCR3 and, to a lesser extent, CCR10, on their surface. The functional consequences of CCL28 deficiency were different between the two infections, as *Ccl28*$^{-/-}$ mice were highly susceptible to *Salmonella* gut infection, but highly resistant to otherwise lethal *Acinetobacter* lung infection. *In vitro*, unstimulated neutrophils harbored pre-formed intracellular CCR3 that was rapidly mobilized to the cell surface following phagocytosis or inflammatory stimuli. Moreover, CCL28 stimulation enhanced neutrophil antimicrobial activity, production of reactive oxygen species, and formation of extracellular traps, all processes that were largely dependent on CCR3. Consistent with the different outcomes in the two infection models, neutrophil stimulation with CCL28 boosted the killing of *Salmonella* but not of *Acinetobacter*. CCL28 thus plays a critical role in the immune response to mucosal pathogens by increasing neutrophil accumulation and activation, which can enhance pathogen clearance but also exacerbate disease depending on the mucosal site and the infectious agent.

Introduction

Chemokines comprise a family of small chemoattractant proteins that play important roles in diverse host processes including chemotaxis, immune cell development, and leukocyte activation (1–3). The chemokine superfamily includes 48 human ligands and 19 receptors, commonly classified into subfamilies (CC, CXC, C, and CX_3C) depending on the location of the cysteines in their sequence (4, 5). Four chemokines predominate in mucosal tissues: CCL25, CCL28, CXCL14, and CXCL17 (6).

56 CCL28, also known as Mucosae-associated Epithelial Chemokine (MEC), belongs to the
57 CC (or β-chemokine) subclass, and is constitutively produced in mucosal tissues including the
58 digestive system, respiratory tract, and female reproductive system (7). Although best studied for
59 its homeostatic functions, CCL28 can also be induced under inflammatory conditions and is thus
60 considered a dual function (homeostatic and inflammatory) chemokine (7).

61 CCL28 signals via two receptors: CCR3 and CCR10 (8). During homeostasis in mice,
62 CCL28 provides a chemotactic gradient for $CCR10^+$ B and T cells and guides the migration of
63 $CCR10^+$ IgA plasmablasts to the mammary gland and other tissues (7, 9, 10). In a disease
64 context, CCL28 has been best studied in allergic airway inflammation. High CCL28 levels are
65 present in airway biopsies from asthma patients (11), and $CCR3^+$ and $CCR10^+$ cells are recruited
66 to the airways in a CCL28-dependent fashion in murine asthma models (12, 13).

67 In the human gut, CCL28 is upregulated during inflammation of the gastric mucosa in
68 *Helicobacter pylori*-infected patients (14) and in the colon of patients with ulcerative colitis, a
69 prominent form of inflammatory bowel disease (15, 16). In the mouse gut, CCL28 production is
70 increased in the dextran sulfate sodium (DSS) model of colitis (10). Epithelial cells are an
71 important source of CCL28 (15, 16), and its expression can be induced by stimulation of cultured
72 airway or intestinal epithelial cells with the proinflammatory cytokines IL-1α, IL-1β, or TNFα, or
73 following *Salmonella* infection of cultured HCA-7 colon carcinoma cells (16).

74 Collectively, a variety of studies have postulated that CCL28 is an important chemokine in
75 inflammatory diseases, ranging from asthma to ulcerative colitis and during the immune response
76 to infection. Yet, CCL28 function remains understudied, largely because *Ccl28*$^{-/-}$ mice have only
77 recently been described (9, 10). Here, we investigate the function and underlying mechanism of
78 CCL28 during the mucosal response to infection.

79 By comparing infection in *Ccl28*$^{-/-}$ mice and their wild-type littermates, we discovered a key
80 role for CCL28 in promoting neutrophil accumulation to the gut during infection with *Salmonella*
81 *enterica* serovar Typhimurium (STm) and to the lung during infection with multidrug-resistant
82 *Acinetobacter baumannii* (Ab). Neutrophils isolated from the infected mucosal sites harbored
83 CCL28 receptors, particularly CCR3, on their surface. *In vitro*, CCR3 was stored intracellularly
84 and was mobilized to the surface upon neutrophil stimulation with proinflammatory molecules or
85 in response to phagocytosis. Neutrophil stimulation of CCL28 resulted in enhanced neutrophil
86 antimicrobial activity against STm, increased production of reactive oxygen species (ROS), and
87 enhanced formation of neutrophil extracellular traps (NETs), all processes that help control
88 infection but also cause extensive tissue damage. We conclude that CCL28 plays a previously
89 unappreciated role in the innate immune response to mucosal pathogens by regulating neutrophil
90 accumulation and activation.

91

92 **Results**

93 **CCL28-mediated responses limit *Salmonella* gut colonization and systemic dissemination.**

94 We investigated CCL28 activity during gastrointestinal infection with the enteric pathogen
95 *Salmonella enterica* serovar Typhimurium (STm) by using the well-established streptomycin-
96 treated C57BL/6 mouse model of colitis (17). At 96h post-infection with STm, we observed a ~4-
97 fold increase of CCL28 by ELISA analysis of feces from wild-type mice relative to uninfected
98 controls (**Fig. 1A**). In a preliminary study, we found that *Ccl28*$^{-/-}$ mice infected with STm exhibited
99 increased lethality compared to their wild-type littermates beginning at 24h post-infection (9). As
100 such, we enumerated STm colony-forming units (CFU) in tissues at 72h post-infection, instead of
101 the frequently studied 96h endpoint. We recovered significantly higher STm CFU from the
102 gastrointestinal tract (cecum content, Peyer's patches), the mesenteric lymph nodes, and

103 systemic sites (bone marrow and spleen) of *Ccl28*$^{-/-}$ mice vs. wild-type littermates (**Fig. 1B**),
104 demonstrating that the chemokine is an essential component of host defense against STm in this
105 colitis model. When bypassing the gut by infecting mice with STm via the intraperitoneal route,
106 we also observed a ~4-fold increase of CCL28 in the serum (**Suppl. Fig. 1A**); however, we
107 recovered equal numbers of STm CFU in the spleen, liver, and blood of wild-type and *Ccl28*$^{-/-}$
108 mice (**Suppl. Fig. 1B**). Thus, CCL28 helps the host to control STm infection at its point of origin
109 in the gut mucosa, prompting us to further investigate the underlying mechanisms of CCL28-
110 mediated mucosal protection.
111
112 **CCL28 promotes neutrophil accumulation to the gut during *Salmonella* infection.**
113 CCL28 has direct antimicrobial activity against some bacteria (e.g., *Streptococcus mutans*
114 and *Pseudomonas aeruginosa*) and fungi (e.g., *Candida albicans*) (18). However, concentrations
115 of CCL28 up to 1μM did not substantially inhibit wild-type STm, whereas the chemokine produced
116 multilog-fold CFU reductions in *Escherichia coli* K12 or an STm Δ*phoQ* mutant, which is more
117 susceptible to antimicrobial peptides than STm wild-type (19), at similar concentrations (**Suppl.
118 Fig. 1C**). Thus direct antimicrobial activity of CCL28 is unlikely to explain the lower STm
119 colonization in wild-type mice in comparison to *Ccl28*$^{-/-}$ mice.
120 During homeostasis, CCL28 exhibits chemotactic activity in the gut mucosa towards CD4^{+}
121 and CD8^{+} T cells and IgA-producing B cells (7, 9, 10). However, B and T cell numbers in the
122 intestine of wild-type and *Ccl28*$^{-/-}$ mice were similar during homeostasis (**Suppl. Fig. 2A** and **2C**)
123 and 48h after STm infection (**Suppl. Fig. 2B** and **2D**), indicating that the chemokine's protective
124 role is likely independent of its B or T cell chemotactic activity. Neutrophils are a crucial component
125 of the host response to STm (reviewed in (20)), and neutropenia increases the severity of infection
126 with non-typhoidal *Salmonella* in both mice and humans (21–24). Strikingly, we isolated ~50%
127 fewer neutrophils (CD11b^{+} Ly6G^{+} cells) from the gut of *Ccl28*$^{-/-}$ mice 48h after STm infection

128 relative to their wild-type littermates (**Fig. 1C, D**). Commensurate with this finding, neutrophil
129 counts in the blood of infected *Ccl28*$^{-/-}$ mice were increased compared to wild-type mice (**Fig. 1C,**
130 **D**), indicating a defect in recruitment of circulating neutrophils to the site of infection. Neutrophil
131 counts in the bone marrow were similar between wild-type and *Ccl28*$^{-/-}$ animals (**Fig. 1C, D**),
132 excluding a defect in granulopoiesis. Likewise, bone marrow and blood neutrophil counts were
133 similar in wild-type and *Ccl28*$^{-/-}$ mice under homeostatic conditions (**Suppl. Fig. 2E, F**) and
134 neutrophils were not found in uninfected gut tissue (data not shown). Thus, CCL28 promotes
135 neutrophil accumulation to the gut during STm infection by a mechanism that transpires after bone
136 marrow neutrophil production and their egress into the blood circulation.

137

138 **Gut proinflammatory gene expression and tissue pathology are reduced in *Ccl28*$^{-/-}$ mice**
139 **infected with STm**

140 Neutrophils can mediate inflammation by directly producing proinflammatory molecules or
141 by engaging in crosstalk with other cells (25). We evaluated the expression of genes encoding
142 proinflammatory cytokines in the cecum of *Ccl28*$^{-/-}$ mice and their wild-type littermates 72h after
143 STm infection. IFNγ and IL-1β gene transcripts were significantly higher in the cecum of infected
144 wild-type mice vs. *Ccl28*$^{-/-}$ mice, while expression of genes encoding other factors involved in
145 neutrophil recruitment (CXCL1, GM-CSF, IL-17A) or the proinflammatory cytokine TNF-α did not
146 differ significantly (**Fig. 1E**). No difference in the expression of these genes was found between
147 uninfected wild-type mice and *Ccl28*$^{-/-}$ mice (data not shown). Consistent with the role of
148 neutrophils as important mediators of inflammation in STm colitis, histopathology at 72h post-
149 infection revealed marked cecal inflammation (including significant neutrophil recruitment) in wild-
150 type mice that was greatly reduced in *Ccl28*$^{-/-}$ mice (**Fig. 1F-H**). Thus, by modulating neutrophil
151 accumulation to the infected gut, CCL28 drives inflammatory tissue pathology and colitis during
152 STm infection.

153

154 ***Ccl28*$^{-/-}$ mice are protected from lethal infection in an *Acinetobacter* pneumonia model**

155 CCL28 is expressed in several mucosal tissues beyond the gut, including the lung (7). To
156 investigate whether CCL28 also promoted neutrophil accumulation and host protection in the lung
157 during infection, we employed a murine *Acinetobacter baumannii (*Ab) pneumonia model (26, 27).
158 Ab is an emerging, frequently multidrug-resistant Gram-negative pathogen that causes potentially
159 lethal nosocomial pneumonia in intensive care unit patients (28). Following intratracheal Ab
160 infection, we observed a striking and unexpected phenotype in the mortality curves of wild-type
161 vs. *Ccl28*$^{-/-}$ mice: while 6 out of 8 wild-type littermates (75%) died within 48h, 7 out of 8 of the
162 *Ccl28*$^{-/-}$ knockout mice (88%) survived through Day 10 post-infection (**Fig. 2A**). The enhanced
163 resistance of *Ccl28*$^{-/-}$ mice relative to their wild-type littermates was not associated with a
164 significant reduction in Ab CFU recovered from bronchoalveolar lavage (BAL) fluid or blood (**Fig.
165 2B, C**). Thus, opposite to what we observed during STm gut infection, CCL28 did not confer
166 protection during Ab lung infection, but rather exacerbated lethality. *In vitro*, high concentrations
167 (1μM) of CCL28 exhibited direct antimicrobial activity against $5x10^5$ CFU of Ab, but not when
168 higher CFU ($5x10^8$/ml) were used as inoculum in the assay (**Suppl. Fig. 1C**). Given that high Ab
169 CFU were recovered in the lung of wild-type mice (**Fig. 2B**), CCL28 does not appear to limit
170 growth of this pathogen *in vivo* even though it exhibits antimicrobial activity *in vitro.* We thus
171 investigated whether there were differences in neutrophil accumulation in the lung between wild-
172 type and *Ccl28*$^{-/-}$ mice that could explain the higher lethality of *Ccl28*$^{-/-}$ mice during Ab lung
173 infection.

174

175 **CCL28 promotes neutrophil accumulation to the lung during *Acinetobacter* infection**

176 Prior studies demonstrated that neutrophils are recruited to the lungs of mice infected with
177 Ab beginning at 4h post-infection, and peak at 24h post-infection (29, 30). As CCL28 contributed
178 to neutrophil recruitment during STm gut infection, we analyzed neutrophil recruitment to the lung
179 mucosa 24h after Ab infection in wild-type and *Ccl28*$^{-/-}$ mice. BAL fluid showed a significantly
180 greater cellular infiltrate (largely comprised of neutrophils; CD11b^{+} Ly6G^{+} cells) in wild-type mice
181 than in *Ccl28*$^{-/-}$ littermates (**Fig. 2D-F**). A similar higher percentage of neutrophils was identified in
182 lung tissue of wild-type mice compared to *Ccl28*$^{-/-}$ mice post-infection, whereas we found no
183 differences in neutrophil numbers in the blood or bone marrow (**Fig. 2E-F**). Although
184 histopathology of lung tissue found substantial lung inflammation in both wild-type and *Ccl28*$^{-/-}$
185 mice after Ab infection (**Fig. 2G**), immunofluorescence analysis revealed remarkable differences
186 in the composition of the cellular infiltrate — lungs from infected wild-type mice showed an
187 abundant infiltrate of neutrophils (Ly6G^{+} cells) that was significantly less in *Ccl28*$^{-/-}$ mice (**Fig. 2H-**
188 **I**).
189
190 Comparable to what we observed during STm gut infection, induction of the genes
191 encoding IFNγ and IL-1β was significantly lower in Ab-infected lungs of *Ccl28*$^{-/-}$ mice relative to
192 wild-type mice (**Fig. 2J**). By contrast, expression of the *Cxcl1* gene was reduced, whereas the
193 other proinflammatory genes tested (*Il17a*, *Csf2*, *Tnfa*) did not differ between the groups (**Fig. 2J**).
194 CCL28 thus contributes to lung inflammation and neutrophil accumulation during Ab pneumonia,
195 which is consistent with our findings during STm gut infection. We thus sought to further
196 investigate how CCL28 regulates neutrophil responses.
197

198 **Gut and BAL neutrophils express receptors CCR3 and CCR10 during infection**

199 CCL28 attracts leukocytes that express at least one of its receptors (CCR3, CCR10).
200 CCR10 is found on T cells, B cells, and IgA-secreting plasma cells, whereas eosinophils express

201 CCR3 (7). Although early studies concluded that CCR3 was absent in neutrophils (31), the
202 receptor was later detected on the surface of neutrophils isolated from patients with chronic
203 inflammation (32). Based on these prior studies and our findings of CCL28-dependent neutrophil
204 accumulation to the gut during gut and lung infection (**Fig. 1, 2**), we performed flow cytometry on
205 single-cell suspensions from tissue isolated from infected mice to evaluate surface expression of
206 CCR3 and CCR10. For mice infected with STm, we analyzed the gut, blood, and bone marrow
207 (**Fig. 3A, B**). While both chemokine receptors were identified on a subset of bone marrow
208 neutrophils (~36% CCR3, ~12% CCR10) and blood neutrophils (~25% CCR3, ~16% CCR10)
209 during infection, neutrophils expressing these receptors were enriched in the inflamed gut, with
210 ~80% expressing CCR3 and ~28% expressing CCR10 (**Fig. 3A**, **B**). In a separate experiment
211 where neutrophils were simultaneously stained for both CCR3 and CCR10, ~35% of gut
212 neutrophils from infected wild-type mice expressed both receptors (**Suppl. Fig. 3A)**, and infected
213 *Ccl28*$^{-/-}$ mice expressed similar levels of these receptors as wild-type mice (**Suppl. Fig. 3B)**.
214 Neutrophils isolated from the BAL of Ab-infected wild-type mice were also positive for
215 CCR3 and CCR10 surface expression, with ~73% of neutrophils expressing CCR3 (**Fig. 3C**) and
216 ~43% expressing CCR10 (**Fig. 3D**). In a separate experiment where neutrophils were
217 simultaneously stained for both CCR3 and CCR10, ~20% of BAL neutrophils from infected wild-
218 type mice expressed both receptors (**Suppl. Fig. 3C)**, and infected *Ccl28*$^{-/-}$ mice expressed similar
219 levels of these receptors as wild-type mice (**Suppl. Fig. 3D)**. As predicted, compared to BAL
220 neutrophils, a lower percentage of neutrophils isolated from the blood and the bone marrow of
221 mice infected with Ab were positive for the receptors (**Fig. 3C, D**). Thus, neutrophils from the
222 infected mucosal tissue expressed high levels of CCL28 receptors, particularly CCR3, and this
223 was associated with higher neutrophil accumulation to the gut during STm colitis and to the lung
224 during Ab pneumonia.
225

226 **Proinflammatory stimuli and phagocytosis induce expression of CCR3 and CCR10 on**
227 **neutrophils**

228 We next investigated potential mechanisms underpinning the upregulation of CCR3 and
229 CCR10 in neutrophils. A prior study indicated that a cocktail of proinflammatory cytokines (GM-
230 CSF, IFNγ, TNFα) boosted CCR3 expression in human peripheral blood mononuclear cells
231 (PBMCs) from healthy donors (32), and expression of these cytokines is highly induced during
232 STm colitis (**Fig. 1E**) and Ab pneumonia (**Fig. 2J**). We thus stimulated bone marrow neutrophils
233 from wild-type mice (which express low levels of CCR3 and CCR10) with these cytokines, and
234 independently with other pro-inflammatory compounds including lipopolysaccharide (LPS), the
235 protein kinase C activator phorbol 12-myristate 13-acetate (PMA), or the N-formylated, bacterial-
236 derived chemotactic peptide fMLP. Treatment of neutrophils with the GM-CSF + IFNγ + TNFα
237 cytokine combination or with LPS induced higher CCR3 (~40% positive cells) and CCR10 (~20%
238 positive cells) expression, whereas PMA and fMLP separately yielded more modest yet significant
239 induction (**Fig. 3E, F**).

240 Phagocytosis of microbes and necrotic debris are critical neutrophil functions at tissue foci
241 of infection and inflammation (33), and gene expression changes are observed in human
242 neutrophils following phagocytosis (34). We thus tested whether CCR3 and CCR10 were induced
243 by phagocytosis, incubating bone marrow neutrophils with latex beads, with or without the
244 aforementioned cytokine cocktail. Although phagocytosis of latex beads alone did not significantly
245 induce neutrophil CCR3 receptor expression (~7% of neutrophils), latex beads augmented with
246 cytokine cocktail induced CCR3 expression (~53% of neutrophils vs. ~30% with cocktail alone;
247 **Fig. 3G**). This synergistic effect of phagocytosis was not noted for CCR10 (**Fig. 3H**).

248 To further probe the role of phagocytosis in CCR3 expression, we incubated bone marrow
249 neutrophils with live STm for 1h. We found that STm rapidly induced the expression of CCR3 on
250 the neutrophil surface (~75% of cells; **Fig. 3I**), whereas CCR10 was only minimally induced (**Fig.**
251 **3J**). Receptor induction was largely blocked by cytochalasin D, a potent inhibitor of the actin

252 polymerization required for phagocytic uptake (**Fig. 3I, J**). Proinflammatory stimuli and
253 phagocytosis thus enhance the expression of CCR3 and, to a lesser extent, CCR10, on the
254 neutrophil surface.
255
256 **CCR3 is stored intracellularly in neutrophils**

257 Neutrophil intracellular compartments and granules harbor enzymes, cytokines, and
258 receptors that are required for rapid responses to pathogens. For example, activation of human
259 neutrophils induces a rapid translocation of complement receptor type 1 (CR1) from an
260 intracellular compartment to the cell surface, increasing its surface expression up to 10-fold (35).
261 As we detected a rapid (within 1h) increase of neutrophil CCR3 surface expression upon STm
262 infection, we hypothesized that CCR3, akin to CR1, may be stored intracellularly in neutrophils,
263 consistent with reports of intracellular CCR3 in eosinophils (36). We found that uninfected bone
264 marrow neutrophils express relatively low surface levels of CCR3 (**Fig. 4A**), but when
265 permeabilized for intracellular staining, most (~83%) were $CCR3^+$, indicating that CCR3 is stored
266 intracellularly (**Fig. 4B**). Upon STm infection *in vitro*, bone marrow neutrophils rapidly increased
267 CCR3 surface expression (up to ~75%; **Fig. 4A**), consistent with a mobilization of pre-formed
268 receptor from an intracellular compartment (**Fig. 4B**). Intracellular stores of CCR10 were also
269 detected in bone marrow neutrophils under homeostatic conditions, with a small but significant
270 increase during STm infection (**Suppl. Fig. 3E**). However, CCR10 was expressed on the surface
271 of only ~1% uninfected bone marrow neutrophils, which increased to ~3% during STm infection
272 (**Suppl. Fig. 3E**). *In vitro*, Ab infection induced higher surface expression of CCR3 on neutrophils
273 (~26%; **Fig. 4C**), whereas CCR10 did not significantly increase (**Suppl. Fig. 3F**). Most bone
274 marrow neutrophils also expressed intracellular CCR3 (**Fig. 4D**) and CCR10 (**Suppl. Fig. 3F**)
275 during Ab infection. Similar to the *in vitro* findings, neutrophils isolated from bone marrow, blood,
276 and gut tissue of mice orally infected with STm, as well as from bone marrow, blood, and BAL

277 fluid of mice infected with Ab, harbored both intracellular and surface CCR3, albeit at differing
278 levels (**Fig. 4E, F**). Of note, CCR3 surface expression levels were higher on neutrophils isolated
279 from the gut and the BAL relative to other sites (**Fig. 4E, F**). We conclude that CCR3 is stored
280 intracellularly in neutrophils and quickly mobilized to the cell surface upon infection, phagocytosis,
281 and/or cytokine stimulation.

282

283 **CCL28 enhances neutrophil antimicrobial activity, ROS production and NET formation via**
284 **CCR3 stimulation.**

285 Chemokines are essential for neutrophil migration to sites of infection and may regulate
286 additional neutrophil bactericidal effector functions including the production of reactive oxygen
287 species (ROS) and formation of neutrophil extracellular traps (NETs) (37). We tested if CCL28
288 has chemotactic and/or immunostimulatory activity towards bone marrow neutrophils *in vitro* after
289 boosting their CCR3 surface expression with the cytokine cocktail (GM-CSF + IFNγ + TNFα)
290 shown in **Fig. 3**. We incubated the neutrophils either with CCL28, or with the well-known
291 neutrophil chemoattractant CXCL1, or with CCL11/eotaxin, a chemokine that binds CCR3 and is
292 induced in the asthmatic lung to promote eosinophil recruitment (38–40). We found CCL28
293 promoted neutrophil chemotaxis, though not as potently as CXCL1, while CCL11 had no
294 significant effect (**Fig. 5A**).

295 To test whether CCL28 stimulation enhanced neutrophil effector function, we incubated
296 STm with bone marrow neutrophils for 2.5h with or without CCL28 (50nM) or CCL11 (50nM), then
297 quantified bacterial killing. Stimulation with CCL28 strongly increased neutrophil bactericidal
298 activity against STm, with clearance of ~40% of the bacterial inoculum, compared to only ~10%
299 clearance seen with unstimulated neutrophils (**Fig. 5B**). Neutrophils stimulated with CCL11
300 displayed an intermediate phenotype (~25% bacterial killing). As expected, neither chemokine
301 exhibited direct antimicrobial activity against STm (**Suppl. Fig. 1D**). In stark contrast to findings

302 with STm, *ex vivo* neutrophil killing of Ab was not significantly enhanced by CCL28 or CCL11
303 treatment (**Fig. 5C**). Thus, even though CCL28 modulates neutrophil accumulation in the lung
304 during Ab infection (**Fig. 2D-J**), a plausible contributing factor to why CCL28 fails to reduce
305 pathogen burden in the lung (**Fig. 2B**) is that CCL28 stimulation does not enhance neutrophil
306 bactericidal activity against Ab.

307 Our data indicate that CCR3 is the CCL28 receptor that is most highly expressed in
308 neutrophils during STm infection (**Fig. 3I and Fig. 4**). We next tested whether the CCL28-
309 mediated increase in neutrophil bactericidal activity could be reversed in the presence of the small
310 molecule SB328437, a CCR3 antagonist (41). SB328437 reversed the effect of both CCL28 and
311 CCL11 on neutrophils, corroborating receptor specificity (**Fig. 5D**). An important mechanism of
312 bacterial killing is the production of ROS (42), a process that is triggered in response to infection
313 and enhanced by proinflammatory stimuli including cytokines and chemokines (43). We measured
314 ROS production by incubating neutrophils with the cell-permeable probe 2',7'-
315 dichlorodihydrofluorescein diacetate (H_2DCFDA), and found that CCL28 stimulation enhanced
316 neutrophil ROS production during STm infection (**Fig. 5E**). Importantly, the increased ROS
317 production triggered by CCL28 was reversed when neutrophils were incubated with an anti-CCR3
318 blocking antibody (**Fig. 5F**), but not with an anti-CCR10 blocking antibody (**Fig. 5G**).

319 In addition to their direct antimicrobial activity, ROS trigger other neutrophil responses,
320 including NET formation (43). NETs can be induced by a variety of stimuli including microbial
321 products, inflammatory cytokines and chemokines, immune complexes and activated platelets
322 (44). To determine whether CCL28 enhances NET formation, we incubated human neutrophils
323 with activated platelets with or without CCL28 and evaluated the formation of DNA-MPO
324 complexes by flow cytometry. Incubation of human neutrophils with activated platelets and CCL28
325 increased the percentage of DNA-MPO complexes compared to neutrophils not stimulated with
326 CCL28 (**Fig 5H, 5I**). The effect of CCL28 on platelet-activated NET formation was largely

327 mediated by CCR3, as incubation with the CCR3 antagonist SB328437 significantly reduced the
328 percentage of neutrophils with DNA-MPO complexes (**Fig 5H, 5I**). In contrast, incubation with the
329 CCR10 antagonist BI-6901 did not significantly reduce NET formation, and incubation with both
330 CCR3 and CCR10 antagonists exhibited a similar effect as the CCR3 antagonist alone (**Fig 5H,**
331 **5I**). Together, these results demonstrate that CCL28 enhances neutrophil ROS production and
332 NET formation primarily in a CCR3-dependent manner.

333

334 **Discussion**

335 The mucosal immune response serves to maintain tissue homeostasis and to protect the
336 host against invading pathogens. Here we discovered that the chemokine CCL28 contributes to
337 neutrophil accumulation and activation in the mucosa in two infection models: gastrointestinal
338 infection with *Salmonella*, and lung infection with *Acinetobacter*.

339 Consistent with our initial observation that *Ccl28*$^{-/-}$ mice exhibit higher lethality during STm
340 infection (9), we found higher intestinal colonization and extraintestinal dissemination of STm in
341 *Ccl28*$^{-/-}$ mice than their wild-type littermates (**Fig. 1**). This beneficial role for CCL28 was negligible
342 when the pathogen was inoculated intraperitoneally to bypass the gut mucosa (**Suppl. Fig. 1**).
343 Although it has been reported that CCL28 exerts direct antimicrobial activity against some
344 bacteria and fungi (18), the chemokine does not directly inhibit STm wild-type *in vitro* (**Suppl. Fig.**
345 **1**). Moreover, even though the CCL28 receptors CCR3 and CCR10 are expressed on eosinophils
346 and on B and T cells (8, 31, 45), none of these cell types appeared to be responsible for the
347 observed protective role of CCL28 during *Salmonella* infection. Eosinophils are not a major
348 component of the host response to *Salmonella*, and we observed comparable numbers of B and
349 T cells in the gut during homeostasis, as well as during *Salmonella* infection, in wild-type and
350 *Ccl28*$^{-/-}$ mice (**Suppl. Fig. 2**).

351 Neutrophils are a hallmark of inflammatory diarrhea. In the *Salmonella* colitis model,
352 neutrophils are rapidly recruited to the gut following infection. We found that neutrophil numbers
353 were significantly reduced in the mucosa of infected *Ccl28*$^{-/-}$ mice relative to wild-type mice (**Fig.**
354 **1**), thereby identifying CCL28 as a key factor for neutrophil accumulation during infection.
355 Neutrophils migrate from the bone marrow to the blood to infected sites following a chemokine
356 gradient (37), and express chemokine receptors CXCR1, CXCR2, CXCR4 and CCR2, as well as
357 CCR1 and CCR6 under certain circumstances (46). CXCR2 is a promiscuous receptor that binds
358 to the chemokines CXCL1, 2, 3, 5, 6, 7, and 8 (47), whereas CXCR1 only binds CXCL6 and
359 CXCL8 (37). Activation of CXCR2 induces mobilization of neutrophils from the bone marrow to
360 the bloodstream and participates in the release of NETs (48). Engagement of CXCR1 and CXCR2
361 also triggers signaling pathways resulting in the production of cytokines and chemokines that
362 amplify neutrophil responses (25). Following extravasation to the site of infection, neutrophils
363 downregulate CXCR2 and upregulate CCR1, 2, and 5, which cumulatively boosts neutrophil ROS
364 production and phagocytic activity (37). Our results indicate that CCL28 contributes to neutrophil
365 accumulation and activation (**Fig. 1**), and that its receptors CCR3 and CCR10 are upregulated in
366 the mucosa during infection, where up to ~75% of neutrophils express surface CCR3 (**Fig. 3**).
367 The reciprocal regulation of CXCR2 and CCR3/CCR10 in neutrophils and each receptor's
368 contribution to neutrophil migration and retention during infectious colitis need to be elucidated by
369 further studies.

370 Although an initial study concluded CCR3 was absent on neutrophils (31), two subsequent
371 studies reported CCR3 expression on human neutrophils isolated from the lung of patients with
372 chronic lung disease (32) and on neutrophils isolated from the BAL fluid of mice infected with
373 influenza (49). CCR10 expression in neutrophils has not been previously reported. Our study
374 demonstrates that a substantial number of neutrophils isolated from infected mucosal sites
375 express CCR3 as well as CCR10 on their surface, whereas resting neutrophils do not express

376 these receptors on their surface (**Fig. 3**). As we detected CCR3 on the neutrophil surface quite
377 rapidly after infection, we predicted that the receptor was stored in intracellular compartments,
378 akin to what was found in eosinophils (36). Indeed, neutrophils isolated from bone marrow, blood,
379 and infected mucosal tissue were all positive for CCR3 intracellular staining (**Fig. 4**), and we could
380 recapitulate the increase of surface receptor expression *in vitro* by incubating bone marrow
381 neutrophils with proinflammatory stimuli (LPS, or the cytokines GM-CSF + IFNγ + TNFα), or
382 following phagocytosis of bacterial pathogens (**Fig. 3**). In all cases, upregulation of surface CCR3
383 on neutrophils was more robust than that of CCR10. CCL28 stimulation of bone marrow
384 neutrophils *in vitro* increased their antimicrobial activity and ROS production when infected with
385 *Salmonella*, which was reverted by blocking CCR3 but not CCR10 (**Fig. 5**). Platelet-activated
386 neutrophils stimulated with CCL28 also showed enhanced NET formation, again largely in a
387 CCR3-dependent fashion (**Fig. 5**). Thus, CCL28 is a potent activator of neutrophils, and it appears
388 to do so primarily via CCR3. Further studies with receptor knock-out mice are needed to determine
389 the contribution of each CCL28 receptor to the *in vivo* phenotypes.

390 A reduction of neutrophil accumulation was also observed in the BAL and lung of *Ccl28*$^{-/-}$
391 mice during *Acinetobacter* infection (**Fig. 2**), and neutrophils recruited to the lung harbored
392 surface CCR3 and CCR10 (**Fig. 3, 4**). However, the functional consequences of CCL28 deficiency
393 was strikingly different in this model, as *Ccl28*$^{-/-}$ mice were protected during Ab pneumonia. Most
394 *Ccl28*$^{-/-}$ mice survived until the experiment's arbitrary endpoint at Day 10 post-infection, whereas
395 nearly all wild-type littermates succumbed by Day 2 (**Fig. 2**). The lung, possessing a thin, single-
396 cell alveolar layer to promote gas exchange, is less resilient than the intestine to neutrophil
397 inflammation before losing barrier integrity and critical functions. Thus, even though insufficient
398 neutrophil recruitment can lead to life-threatening infection, extreme accumulation of neutrophils
399 can result in excessive inflammatory lung injury (50). The high survival of *Ccl28*$^{-/-}$ mice infected
400 with Ab indicates that CCL28 may be detrimental for the host at least in the context of some

401 pulmonary infection. While functioning neutrophils have been described to play a role in
402 controlling *Acinetobacter* infection (29, 51, 52), an exaggeration of neutrophil recruitment to the
403 *Acinetobacter*-infected lung is deleterious (53–55). For example, in one relevant *Acinetobacter*
404 pneumonia study, depletion of alveolar macrophages increased neutrophil infiltration, promoted
405 extensive tissue damage, and increased systemic dissemination of *Acinetobacter* (56). Of note,
406 in contrast to *Salmonella*, stimulation with CCL28 did not enhance neutrophil antimicrobial activity
407 against *Acinetobacter*, which may partly explain the lack of a CCL28-mediated protective
408 response (**Fig. 5**). The bacteriological mechanism(s) by which *Acinetobacter* may be resistant to
409 CCL28-dependent neutrophil antimicrobial responses require further investigation.

410 Even though CCL28 exhibited direct antimicrobial activity against *Acinetobacter*, higher
411 concentrations of CCL28 (1μm) are needed for protection, and even so are not sufficient against
412 higher pathogen burden (**Suppl. Fig. 1**). Our findings are consistent with prior studies showing
413 that the impact of the host response to infection can be context dependent, and that some immune
414 components mediate different outcomes in the gut and in the lung. For example, *Cxcr2*$^{-/-}$ mice
415 exhibit a defect in neutrophil recruitment that is detrimental during *Salmonella* infection (57), but
416 protective during lung infection with *Mycobacterium tuberculosis*, due to reduced neutrophil
417 recruitment and reduced pulmonary inflammation (58). Similarly, CCL28-dependent modulation
418 of neutrophil accumulation and activation during infection can be protective or detrimental
419 depending on the pathogen and on the site of infection.

420 Altogether, this study demonstrates that CCL28 plays an important role in the mucosal
421 response to pathogens through neutrophil accumulation to the site of infection, that neutrophils
422 isolated from the infected mucosa express the CCL28 receptors CCR3 and CCR10, and that
423 CCL28 enhances neutrophil activation, ROS production and NET formation, primarily through
424 CCR3. These findings could have implications for other infectious and non-infectious diseases

425 where neutrophil recruitment plays a major role, and may lead to the identification of new CCL28-
426 targeted therapies to modulate neutrophil function and mitigate collateral damage.

427

428 **Materials and methods**

429 **Generation and breeding of *Ccl28*$^{-/-}$ mice**

430 The first colony of *Ccl28*$^{-/-}$ mice was described in a prior manuscript (9) and used for initial studies
431 at UC Irvine. At UC San Diego, we generated a new colony of *Ccl28*$^{-/-}$ mice with Cyagen
432 Biosciences (Santa Clara, California), using CRISPR/CAS9 technology. Exons 1 and 3 were
433 selected as target sites, and two pairs of gRNA targeting vectors were constructed and confirmed
434 by sequencing. The gRNA and Cas9 mRNA were generated by *in vitro* transcription, then co-
435 injected into fertilized eggs for knockout mouse production. The resulting pups (F0 founders) were
436 genotyped by PCR and confirmed by sequencing. F0 founders were bred to wild-type mice to test
437 germline transmission and for F1 animal generation. Tail genotyping of offspring was performed
438 using the following primers:

439 F: 5'-TCATATACAGCACCTCACTCTTGCCC-3', R: 5'-GCCTCTCAAAGTCATGCCAGAGTC-3'
440 and He/Wt-R: 5'-TCCCGGCCTTGAGTATGTTAGGC-3'. The expected product size for the wild-
441 type allele is 466 bp and for the knockout allele is 700 bp.

442 All mouse experiments were conducted with cohoused wild-type and *Ccl28*$^{-/-}$ littermate mice, and
443 were reviewed and approved by the Institutional Animal Care and Use Committees at UC Irvine
444 and UC San Diego.

445

446 ***Salmonella* infection models**

447 For the *Salmonella* colitis model, 8-10 week-old male and female mice were orally gavaged with
448 20mg streptomycin 24h prior to oral gavage with 10^9 colony-forming units (CFU) of *Salmonella*
449 *enterica* serovar Typhimurium strain IR715 (a fully virulent, nalidixic acid-resistant derivative of
450 ATCC 14028s) (59), as previously described (17, 60). Mice were euthanized at 72h post-infection,
451 then colon content, spleen, mesenteric lymph nodes, Peyer's patches, and bone marrow were
452 collected, weighed, homogenized, serially diluted, and plated on Miller Lysogeny broth (LB) + NaI
453 (50µg/mL) agar plates to enumerate *Salmonella* CFU. For the *Salmonella* bacteremia model, mice
454 were injected intraperitoneally with 10^3 CFU. Mice were euthanized at 72h post-infection, then
455 blood, spleen, and liver were collected to determine bacterial counts.

456

457 ***Acinetobacter* infection model**

458 For the murine pneumonia model**,** *Acinetobacter baumannii* strain AB5075 was cultured in Cation-
459 Adjusted Mueller-Hinton Broth (CA-MHB) overnight, then subcultured the next day to an OD_{600} of
460 ~0.4 ($1x10^8$ CFU/mL; mid-logarithmic phase). These cultures were centrifuged at 3202x*g*, the
461 supernatant was removed, and pellets were resuspended and washed in an equal volume of 1x
462 Dulbecco's PBS (DPBS) three times. The final pellet was resuspended in 1x DPBS to yield a
463 suspension of 2.5×10^9 CFU/mL. Using an operating otoscope (Welch Allyn), mice under 100
464 mg/kg ketamine (Koetis) + 10 mg/kg xylazine (VetOne) anesthesia were inoculated intratracheally
465 with 40 µL of the bacterial suspension (10^8 CFU/mouse). Post-infection mice were recovered on
466 a sloped heating pad. For analysis of bacterial CFU, mice were sacrificed at 24h post-infection,
467 the BAL was collected, and serial dilutions were plated on LB agar to enumerate bacteria (26).

468

469 **CCL28 ELISA**

470 Fresh fecal samples were collected at 96h post-infection from wild-type mice. Fecal pellets were
471 weighed, resuspended in 1 mL of sterile PBS containing a protease inhibitor cocktail (Roche),
472 and incubated at room temperature shaking for 30 min. Samples were centrifuged at 9391 x *g* for
473 10 min, supernatants were collected, then analyzed to quantify CCL28 using a sandwich ELISA
474 kit (BioLegend).
475
476 **Cell extraction and analysis**

477 For the *Salmonella* colitis model, the terminal ileum, cecum, and colon were collected at 48h post-
478 infection. All tissues were kept in IMDM medium supplemented with 10% FBS and 1%
479 antibiotic/antimycotic. Next, the Peyer's patches were removed, and the intestinal fragments were
480 cut open longitudinally and washed with HBSS supplemented with 15 mM HEPES and 1%
481 antibiotic/antimycotic. Then, the tissue was shaken in 10 mL of an HBSS/ 15 mM HEPES/ 5 mM
482 EDTA/ 10% FBS solution at 37 ºC in a water bath for 15 min. The supernatant was removed and
483 kept on ice. The remaining tissue was cut into small pieces and digested in a 10 mL mixture of
484 collagenase (Type VII, 1 mg/mL), Liberase (20 µg/mL), and DNAse (0.25 mg/mL) in IMDM
485 medium for 15 min in a shaking water bath at 37 ºC. Afterwards, the supernatant and tissue
486 fractions were strained through a 70 µm cell strainer and pooled, and the extracted cells were
487 used for flow cytometry staining. For the *A. baumannii* infection model, the lungs were collected
488 and processed as described for the gut. BAL was collected, centrifuged, and pellets were washed
489 with 1x PBS. The obtained cells were used for flow cytometry staining. Briefly, cells were blocked
490 with a CD16/32 antibody (Bio-Legend), stained with the viability dye eFluor780 (Thermo Fisher),
491 then extracellularly stained using the following monoclonal antibodies: anti-mouse CD45 (clone
492 30-F11), anti-mouse CD3 (clone 17A2), anti-mouse CD4 (clone RM4-5), anti-mouse CD8α (clone
493 53-6.7), anti-mouse CD19 (clone 1D3/CD19), anti-mouse Ly6G (clone 1A8), anti-mouse CD11b
494 (clone M1/70) from BioLegend; anti-mouse CCR3 (clone FAB729P) and anti-mouse CCR10

495 (clone FAB2815A) from R&D Systems. After staining, cells were fixed for 20 min with 4%
496 paraformaldehyde (Fixation buffer; BioLegend). When intracellular staining was performed, cells
497 were permeabilized (Permeabilization buffer; BioLegend), and the staining was performed in the
498 same buffer following the manufacturer's instructions. Cells were analyzed on an LSRII flow
499 cytometer (BD Biosciences) and the collected data were analyzed with FlowJo v10 software
500 (TreeStar). For analysis of human neutrophils, whole-blood samples were collected in
501 ethylenediaminetetraacetic acid (EDTA) for cellular analyses. Whole blood cell staining was
502 performed using an Fc receptor blocking solution (Human TruStain FcX; BioLegend), the viability
503 dye eFluor780 (Thermo Fisher), and the following conjugated monoclonal antibodies:
504 PerCP/Cy5.5 anti-human CD45 antibody (clone HI30), Pacific Blue anti-mouse/human CD11b
505 antibody (clone M1/70), FITC anti-human CD62L antibody (clone DREG-56), from BioLegend;
506 PE anti-human CCR3 antibody (clone 61828), and APC anti-human CCR10 antibody (clone
507 314305) from R&D Systems. Samples were analyzed by flow cytometry using an LSR Fortessa
508 flow cytometer (BD Biosciences), and data was analyzed using FlowJo v10 software.

509

510 ***In vitro* neutrophil stimulation**

511 Neutrophils were obtained from the bone marrow of C57BL/6 wild-type mice using the EasySep
512 Mouse Enrichment Kit (STEMCELL), following the manufacturer's instructions. After enrichment,
513 $1x10^6$ neutrophils were seeded in a round-bottom 96-well plate with RPMI media supplemented
514 with 10% FBS, 1% antibiotic/antimycotic mix, and HEPES (1mM) (Invitrogen). For stimulation,
515 cells were incubated with the following concentrations of recombinant mouse cytokines: TNFα
516 (100 ng/mL), IFNγ (500 U/mL) and GM-CSF (10 ng/mL), all from R&D systems. Recombinant
517 cytokines were added alone or in combination. For indicated experiments, polystyrene beads
518 (Thermo Fisher) were added to neutrophils at a 1:1 ratio. Cells were incubated for 4 hours at 37

519 ºC and 5% CO_2. After incubation, cells were recovered by centrifugation, washed with PBS, and
520 processed for flow cytometry as described above.

521

522 **Chemotaxis assay**

523 Enriched neutrophils from the bone marrow of wild-type mice were stimulated with a cocktail of
524 mouse recombinant cytokines (TNFα, IFNγ, GM-CSF), as described above, to induce receptor
525 expression. After stimulation, cells were washed twice with PBS, resuspended in RPMI media
526 supplemented with 0.1% BSA (w/v) to a final concentration of $1x10^7$ cells/mL, and 100 µL of the
527 cell suspension were placed in the upper compartment of a Transwell chamber (3.0 µm pore size;
528 Corning Costar). 50 nM of recombinant mouse CCL28, CCL11 (R&D Systems), or CXCL1
529 (Peprotech) were placed into the lower compartment of a Transwell chamber. The Transwell plate
530 was then incubated for 2h at 37 ^oC. The number of cells that migrated to the lower compartment
531 was determined by flow cytometry. The neutrophil chemotaxis index was calculated by dividing
532 the number of cells that migrated in the presence of a chemokine by the number of cells that
533 migrated in control chambers without chemokine stimulation.

534

535 **Neutrophil *in vitro* infection and bacterial killing assays**

536 Bone marrow neutrophils were obtained from mice as described above. *S.* Typhimurium and *A.*
537 *baumannii* were grown as described in the respective mouse experiment sections. For STm
538 infection, bacteria were then opsonized with 20% normal mouse serum for 30 min at 37 ^oC. After
539 neutrophils were enriched, $1x10^6$ neutrophils were seeded in a round-bottom 96-well plate with
540 RPMI media supplemented with FBS (10%), and bacteria were added at a multiplicity of infection
541 (MOI)= 10. The plate was centrifuged to ensure interaction between cells and bacteria. After 30
542 min of contact with STm, the media was changed and RPMI media supplemented with FBS (10%)

543 and gentamicin (100 µg/mL) was added, and cells were incubated for 30 min more. For Ab
544 infection, $1x10^6$ neutrophils were seeded in a round-bottom 96-well plate with RPMI media
545 supplemented with FBS (10%), and bacteria were added at a multiplicity of infection (MOI)= 10.
546 The plate was centrifuged to ensure interaction between cells and bacteria, and cells were
547 incubated for 4 h at 37 ^oC and 5% CO2. For analysis of CCR3 and CCR10 expression, cells were
548 recovered by centrifugation, washed with PBS, and processed for flow cytometry as described
549 above. For inhibition of phagocytosis, bone marrow neutrophils were pre-incubated with
550 cytochalasin D (10 µM) in DMSO (0.1%), or DMSO (vehicle), for 30 min prior to infection with
551 opsonized *S*. Typhimurium for 1h at an MOI=10. For killing assays, recombinant mouse CCL28
552 (50nM) (45) and CCL11 (25nM) (61) (R&D systems) were added to neutrophils. When indicated,
553 the CCR3 receptor antagonist SB328437 (Tocris Bioscience) was added at a final concentration
554 of 10 µM (41). Neutrophils infected with STm were incubated for 2.5h and neutrophils infected
555 with *A. baumannii* were incubated for 4.5h at 37 ^oC and 5% CO_2. After incubation, 1:2 dilution was
556 performed with PBS supplemented with 2% Triton X-100 and then serial dilution was performed
557 and plated on LB agar to enumerate bacteria. To calculate the percentage of bacterial survival,
558 the number of bacteria recovered in the presence of neutrophils was divided by the number of
559 bacteria recovered from wells that contained no neutrophils, then multiplied by 100.

560

561 **Reactive oxygen species (ROS) production**

562 Neutrophils were obtained from the bone marrow of C57BL/6 wild-type mice using the EasySep
563 Mouse Enrichment Kit (STEMCELL Technologies), following the manufacturer's instructions.
564 After enrichment, 2.5 x 10^6 cells/mL were resuspended in phenol red-free RPMI media (Gibco)
565 supplemented with 10% FBS (Gibco), and HEPES (1mM, Invitrogen). The cells were incubated
566 in presence of 2',7'-dichlorodihydrofluorescein diacetate (H_2DCFDA, 25 mM) (Invitrogen) for
567 30min at 37 ºC and 5% of CO_2, as previously described (62). After incubation with H_2DCFDA,

568 neutrophils were infected with STm as described above, then incubated for 4h with mouse
569 recombinant CCL28 (50 nM), anti-mouse CCR3 antibody (5 mg/1x10^6 cells, clone 83103), anti-
570 mouse CCR10 antibody (5 mg/1x10^6 cells, clone 248918) or anti-rat IgG2A (5 mg/1x10^6 cells,
571 clone 54447), all from R&D Systems. Neutrophils were analyzed by flow cytometry to determine
572 ROS production using a BD FACSCanto flow cytometer, and data was analyzed using the FlowJo
573 v10 software.
574
575 **Neutrophil extracellular traps (NETs) production**
576
577 Whole-blood samples were collected from healthy donors recruited at a tertiary care center in
578 Mexico City (Instituto Nacional de Ciencias Médicas y Nutrición Salvador Zubirán). Healthy
579 donors signed an informed consent form before inclusion in the study, and the protocol was
580 approved by the Instituto Nacional de Ciencias Médicas y Nutrición Salvador Zubirán ethics and
581 research committees (Ref. 3341) in compliance with the Helsinki declaration. Neutrophils were
582 obtained from peripheral blood of healthy voluntary donors using the EasySep Direct Human
583 Neutrophil Isolation Kit (STEMCELL Technologies), following the manufacturer's instructions. In
584 parallel, platelets from human peripheral blood were isolated as described (63). Briefly, whole
585 blood was centrifuged at 200*g* for 10 minutes at 4 ºC, and plasma was recovered and then
586 centrifuged again at 1550*g* for 10 minutes at 4 ºC. The cell pellet was resuspended in RPMI media
587 supplemented with 10% FBS (4 x 10^7 cells/mL) and then incubated with LPS (5 mg/mL) for 30
588 minutes at 37 ºC to induce platelet activation (64). Subsequently, neutrophils were incubated with
589 autologous activated platelets (1:10 ratio) (65) for 2.5h and human recombinant CCL28 (50 nM)
590 (BioLegend), the CCR3 antagonist SB328437 (10 mM, Tocris Bioscience) and/or the CCR10
591 antagonist BI-6901 (20 mM, Boehringer-Ingelheim) were added as indicated. Cells were then
592 incubated with the DNA-binding dye Helix-NP Green (10 nM, BioLegend), human anti-
593 myeloperoxidase (MPO)-Biotin antibody (clone MPO421-8B2, Novus Biologicals), and APC/Cy7

594 streptavidin (BioLegend). Samples were analyzed using an LSR Fortessa flow cytometer (BD
595 Biosciences) to determine the presence of DNA-MPO complexes (66), and data were analyzed
596 using FlowJo v10 software.

597

598 **Growth of bacteria in media supplemented with recombinant chemokines**

599 *S.* Typhimurium wild-type, *S.* Typhimurium *phoQ* mutant, and *Escherichia coli* K12 were grown in
600 LB broth overnight at 37 °C. *Acinetobacter baumannii* was cultured in Cation-Adjusted Mueller-
601 Hinton Broth (CA-MHB) under the same conditions. The following day, cultures were diluted 1:100
602 in LB and grown at 37 °C for 3 hr, subsequently diluted to ~0.5 x 10^6 CFU/mL or ~0.5 x 10^9
603 CFU/mL in 1 mM potassium phosphate buffer (pH 7.2), then incubated at 37 °C in the presence
604 or absence of recombinant murine CCL28 (BioLegend) at the indicated concentrations. After 2h,
605 samples were plated onto LB agar to enumerate viable bacteria. In other assays, *S.* Typhimurium
606 was grown as described above and ~1x10^7 CFU/mL were incubated at 37 °C for 2.5h in the
607 presence or absence of recombinant murine CCL28 (50 nM) (45) or CCL11 (25 nM) (61) in RPMI
608 medium supplemented with 10% FBS. After incubation, samples were plated onto LB + NaI agar
609 to enumerate viable bacteria.

610

611 **RNA extraction and qPCR**

612 Total RNA was extracted from mouse cecal or lung tissue using Tri-Reagent (Molecular Research
613 Center). Reverse transcription of 1 µg of total RNA was performed using the SuperScript VILO
614 cDNA Synthesis kit (Thermo Fisher Scientific). Quantitative real-time PCR (qRT-PCR) for the
615 expression of *Actb* (β-actin), *Cxcl1, Tnfa, Ifng, Csf2, Il1b,* and *Il17a* was performed using the
616 PowerUp SYBR Green Master Mix (Applied Biosystems) on a QuantStudio 5 Real-Time PCR
617 System (Thermo Fisher Scientific). Gene expression was normalized to *Actb* (β-actin). Fold

618 changes in gene expression were relative to uninfected controls and calculated using the *ΔΔ*Ct
619 method.

620

621 **Histopathology**

622 Cecal and lung tissue samples were fixed in 10% buffered formalin, embedded in paraffin
623 according to standard procedures, and sectioned at 5 µm. Pathology scores of cecal and lung
624 samples were determined by blinded examinations of hematoxylin and eosin (H&E)-stained
625 sections. Each cecal section was evaluated using a semiquantitative score as described
626 previously (67). Lung inflammation was assessed by a multiparametric scoring based on previous
627 work (68).

628

629 **Immunofluorescence**

630 Deparaffinized lung sections were stained with a purified rat anti-mouse Ly6G antibody (clone
631 1A8, BioLegend) according to standard immunohistochemical procedures. Ly6G+ cells were
632 visualized by a goat anti-rat secondary antibody (Invitrogen). Cell nuclei were stained with DAPI
633 in SlowFade Gold Antifade Mountant (Invitrogen). Slides were scanned on a Zeiss Axio Scan.Z1
634 slide scanner and whole lung scans were evaluated with QuPath analysis software (69). Ly6G+
635 cells per mouse were quantified by averaging the neutrophil numbers of 3 consecutive high-power
636 fields in regions with moderate to severe inflammation.

637

638 **Statistical analysis**

639 Statistical analysis was performed with GraphPad Prism 9. CFU data, percentage of $CCR3^+$ or
640 $CCR10^+$ neutrophils *in vivo* and *in vitro*, and data from functional neutrophil assays were
641 transformed to Log10 and passed a normal distribution test before running statistical analyses.

642 CFU from *in vivo* infection experiments, cytokine secretion, qPCR data, and neutrophils numbers
643 were compared by Mann-Whitney U test. Survival curves were compared by the Log-rank
644 (Mantel-Cox) test. Data that were normally distributed were analyzed by one-way ANOVA for
645 independent samples or paired samples, depending on the experimental setup. Dunnett's multiple
646 comparisons test was applied when we compared the different conditions to a single control
647 group, while Tukey's multiple comparison test was performed when we compared each condition
648 with each other. Greenhouse-Geisser correction was applied when there were differences in the
649 variance among the groups. Data from chemokine migration were analyzed by a non-parametric
650 ANOVA (Kruskal-Wallis's test), assuming non-equal SD given the differences in the variance
651 among the groups and followed by Dunn's multiple comparisons test. Paired *t* test was used when
652 only two paired experimental groups were compared. A p value equal to or below 0.05 was
653 considered statistically significant. * indicates an adjusted p value ≤0.05, ** p value ≤0.01, *** p
654 value ≤0.001, **** p value ≤0.0001.
655
656
657
658 **Acknowledgements**
659 This work was supported by the NIH (Public Health Service Grants AI121928) to MR, by a pilot
660 project award from the NIAID Mucosal Immunology Studies Team (MIST) to APL, and by a grant
661 from the InnovaUNAM of the National Autonomous University of Mexico (UNAM) and Alianza
662 UCMX of the University of California, to APL and MR. RRG was partly supported by a fellowship
663 from the Max Kade Foundation and by a fellowship from the Crohn's and Colitis Foundation. MHL
664 was partly supported by NIH training grant T32 DK007202. ND was supported by NIH training
665 grant NIH 5T32HD087978-05 and NIH NIAID grant 1-U01-AI124316. GTW was supported by NIH
666 training grant T32AI007036. KM was partly supported by São Paulo Research Foundation
667 (FAPESP) Grants 2019/14833-0 and 2018/22042-0. RCD, SR-R, and VAS-H were supported by

a Grad School Fellowship from CONACyT. MR and VN are supported by Public Health Service Grant AI145325. Work in JLM-M lab was supported by CONACyT-FOSISS grant A3-S-36875 and UNAM-DGAPA-PAPIIT Program grant IN213020. Work in MR lab is also supported by NIH Grants AI126277, AI145325, AI154644, AI096528, and by the Chiba University-UCSD Center for Mucosal Immunology, Allergy, and Vaccines. MR holds an Investigator in the Pathogenesis of Infectious Disease Award from the Burroughs Wellcome Fund. We would like to thank Dr. Albert Zlotnik for his thoughtful suggestions on the project over the years. We also acknowledge Boehringer-Ingelheim Pharma GmbH & Co. KG for the kind gift of the CCR10 antagonist BI-6901, and the Histology Core at the La Jolla Institute for Immunology.

Author contributions

APL and MR conceived the overall study. APL, SS, MHL, ND, SLB, RRG, KM, GTW, S-PN, VN, JLM-M, and MR designed the experiments and analyzed the data. APL, SS, MHL, ND, SLB, RRG, KM, GTW, VAS-H, RC-D, and SR-R performed experiments. RRG analyzed the histopathology. APL, S-PN, VN, and MR wrote the paper. APL, S-PN, VN, and MR provided supervision and funding support.

References

1. A. Zlotnik, O. Yoshie, Chemokines: a new classification system and their role in immunity. *Immunity* **12**, 121–127 (2000).

2. A. Zlotnik, A. M. Burkhardt, B. Homey, Homeostatic chemokine receptors and organ-specific metastasis. *Nat. Rev. Immunol.* **11**, 597–606 (2011).

3. I. F. Charo, R. M. Ransohoff, The many roles of chemokines and chemokine receptors in inflammation. *N. Engl. J. Med.* **354**, 610–621 (2006).

4. H. Nomiyama, N. Osada, O. Yoshie, Systematic classification of vertebrate chemokines based on conserved synteny and evolutionary history. *Genes Cells* **18**, 1–16 (2013).

5. C. E. Hughes, R. J. B. Nibbs, A guide to chemokines and their receptors. *FEBS J.* **285**, 2944–2971 (2018).

697 6. M. Hernández-Ruiz, A. Zlotnik, Mucosal Chemokines. *J. Interferon Cytokine Res.* **37**, 62–
698 70 (2017).

699 7. T. Mohan, L. Deng, B.-Z. Wang, CCL28 chemokine: An anchoring point bridging innate and
700 adaptive immunity. *Int. Immunopharmacol.* **51**, 165–170 (2017).

701 8. J. Pan, *et al.*, Cutting Edge: A Novel Chemokine Ligand for CCR10 And CCR3 Expressed
702 by Epithelial Cells in Mucosal Tissues. *The Journal of Immunology* **165**, 2943–2949 (2000).

703 9. A. M. Burkhardt, *et al.*, CCL28 Is Involved in Mucosal IgA Responses, Olfaction, and
704 Resistance to Enteric Infections. *J. Interferon Cytokine Res.* **39**, 214–223 (2019).

705 10. K. Matsuo, *et al.*, CCL28-Deficient Mice Have Reduced IgA Antibody-Secreting Cells and
706 an Altered Microbiota in the Colon. *J. Immunol.* **200**, 800–809 (2018).

707 11. M. T. O'Gorman, N. A. Jatoi, S. J. Lane, B. P. Mahon, IL-1beta and TNF-alpha induce
708 increased expression of CCL28 by airway epithelial cells via an NFkappaB-dependent
709 pathway. *Cell. Immunol.* **238**, 87–96 (2005).

710 12. A. E. John, M. S. Thomas, A. A. Berlin, N. W. Lukacs, Temporal production of CCL28
711 corresponds to eosinophil accumulation and airway hyperreactivity in allergic airway
712 inflammation. *Am. J. Pathol.* **166**, 345–353 (2005).

713 13. K. English, C. Brady, P. Corcoran, J. P. Cassidy, B. P. Mahon, Inflammation of the
714 respiratory tract is associated with CCL28 and CCR10 expression in a murine model of
715 allergic asthma. *Immunol. Lett.* **103**, 92–100 (2006).

716 14. M. Hansson, *et al.*, CCL28 is increased in human Helicobacter pylori-induced gastritis and
717 mediates recruitment of gastric immunoglobulin A-secreting cells. *Infect. Immun.* **76**, 3304–
718 3311 (2008).

719 15. D. S. Lee, *et al.*, Expression of Chemokine CCL28 in Ulcerative Colitis Patients. *Gut Liver*
720 (2020) https:/doi.org/10.5009/gnl19273.

721 16. H. Ogawa, M. Iimura, L. Eckmann, M. F. Kagnoff, Regulated production of the chemokine
722 CCL28 in human colon epithelium. *Am. J. Physiol. Gastrointest. Liver Physiol.* **287**, G1062-
723 9 (2004).

724 17. M. Barthel, *et al.*, Pretreatment of mice with streptomycin provides a Salmonella enterica
725 serovar Typhimurium colitis model that allows analysis of both pathogen and host. *Infect.*
726 *Immun.* **71**, 2839–2858 (2003).

727 18. K. Hieshima, *et al.*, CCL28 has dual roles in mucosal immunity as a chemokine with broad-
728 spectrum antimicrobial activity. *J. Immunol.* **170**, 1452–1461 (2003).

729 19. E. A. Groisman, The pleiotropic two-component regulatory system PhoP-PhoQ. *J.*
730 *Bacteriol.* **183**, 1835–1842 (2001).

731 20. A. Perez-Lopez, J. Behnsen, S.-P. Nuccio, M. Raffatellu, Mucosal immunity to pathogenic
732 intestinal bacteria. *Nat. Rev. Immunol.* **16**, 135–148 (2016).

733 21. F. N. Bhatti, I. A. Burney, M. I. Moid, T. Siddiqui, Bacterial isolates from neutropenic febrile
734 pediatric patients and their sensitivity patterns to antibiotics. *J. Pak. Med. Assoc.* **48**, 287–

735 290 (1998).

736 22. Y. Yaman, *et al.*, Non-typhoidal Salmonella bacteraemia in paediatric leukaemia patients.
737 *Contemp. Oncol.* **22**, 105–107 (2018).

738 23. A. P. Vassiloyanakopoulos, S. Okamoto, J. Fierer, The crucial role of polymorphonuclear
739 leukocytes in resistance to Salmonella dublin infections in genetically susceptible and
740 resistant mice. *Proc. Natl. Acad. Sci. U. S. A.* **95**, 7676–7681 (1998).

741 24. J. Fierer, Polymorphonuclear leukocytes and innate immunity to Salmonella infections in
742 mice. *Microbes Infect.* **3**, 1233–1237 (2001).

743 25. I. Sabroe, E. C. Jones, M. K. B. Whyte, S. K. Dower, Regulation of human neutrophil
744 chemokine receptor expression and function by activation of Toll-like receptors 2 and 4.
745 *Immunology* **115**, 90–98 (2005).

746 26. N. Dillon, *et al.*, Surprising synergy of dual translation inhibition vs. Acinetobacter
747 baumannii and other multidrug-resistant bacterial pathogens. *EBioMedicine* **46**, 193–201
748 (2019).

749 27. L. Lin, *et al.*, Azithromycin Synergizes with Cationic Antimicrobial Peptides to Exert
750 Bactericidal and Therapeutic Activity Against Highly Multidrug-Resistant Gram-Negative
751 Bacterial Pathogens. *EBioMedicine* **2**, 690–698 (2015).

752 28. C. Ayoub Moubareck, D. Hammoudi Halat, Insights into Acinetobacter baumannii: A
753 Review of Microbiological, Virulence, and Resistance Traits in a Threatening Nosocomial
754 Pathogen. *Antibiotics (Basel)* **9** (2020).

755 29. H. Van Faassen, *et al.*, Neutrophils play an important role in host resistance to respiratory
756 infection with Acinetobacter baumannii in mice. *Infect. Immun.* **75**, 5597–5608 (2007).

757 30. T. Tsuchiya, *et al.*, NK1. 1+ cells regulate neutrophil migration in mice with Acinetobacter
758 baumannii pneumonia. *Microbiol. Immunol.* **56**, 107–116 (2012).

759 31. R. Höchstetter, *et al.*, The CC chemokine receptor 3 CCR3 is functionally expressed on
760 eosinophils but not on neutrophils. *Eur. J. Immunol.* **30**, 2759–2764 (2000).

761 32. D. Hartl, *et al.*, Infiltrated neutrophils acquire novel chemokine receptor expression and
762 chemokine responsiveness in chronic inflammatory lung diseases. *J. Immunol.* **181**, 8053–
763 8067 (2008).

764 33. E. Uribe-Querol, C. Rosales, Phagocytosis: Our Current Understanding of a Universal
765 Biological Process. *Front. Immunol.* **11**, 1066 (2020).

766 34. S. D. Kobayashi, J. M. Voyich, C. L. Buhl, R. M. Stahl, F. R. DeLeo, Global changes in
767 gene expression by human polymorphonuclear leukocytes during receptor-mediated
768 phagocytosis: cell fate is regulated at the level of gene expression. *Proc. Natl. Acad. Sci. U.*
769 *S. A.* **99**, 6901–6906 (2002).

770 35. M. Berger, E. M. Wetzler, E. Welter, J. R. Turner, A. M. Tartakoff, Intracellular sites for
771 storage and recycling of C3b receptors in human neutrophils. *Proc. Natl. Acad. Sci. U. S. A.*
772 **88**, 3019–3023 (1991).

773 36. L. A. Spencer, *et al.*, Cytokine receptor-mediated trafficking of preformed IL-4 in eosinophils
774 identifies an innate immune mechanism of cytokine secretion. *Proc. Natl. Acad. Sci. U. S.*
775 *A.* **103**, 3333–3338 (2006).

776 37. A. Capucetti, F. Albano, R. Bonecchi, Multiple Roles for Chemokines in Neutrophil Biology.
777 *Front. Immunol.* **11**, 1259 (2020).

778 38. D. M. Conroy, T. J. Williams, Eotaxin and the attraction of eosinophils to the asthmatic lung.
779 *Respir. Res.* **2**, 150–156 (2001).

780 39. E. A. Garcia-Zepeda, *et al.*, Human eotaxin is a specific chemoattractant for eosinophil cells
781 and provides a new mechanism to explain tissue eosinophilia. *Nat. Med.* **2**, 449–456
782 (1996).

783 40. M. Kitaura, *et al.*, Molecular cloning of human eotaxin, an eosinophil-selective CC
784 chemokine, and identification of a specific eosinophil eotaxin receptor, CC chemokine
785 receptor 3. *J. Biol. Chem.* **271**, 7725–7730 (1996).

786 41. J. R. White, *et al.*, Identification of potent, selective non-peptide CC chemokine receptor-3
787 antagonist that inhibits eotaxin-, eotaxin-2-, and monocyte chemotactic protein-4-induced
788 eosinophil migration. *J. Biol. Chem.* **275**, 36626–36631 (2000).

789 42. F. C. Fang, Antimicrobial actions of reactive oxygen species. *MBio* **2** (2011).

790 43. G. T. Nguyen, E. R. Green, J. Mecsas, Neutrophils to the ROScue: Mechanisms of NADPH
791 Oxidase Activation and Bacterial Resistance. *Front. Cell. Infect. Microbiol.* **7**, 373 (2017).

792 44. S. Boeltz, *et al.*, To NET or not to NET:current opinions and state of the science regarding
793 the formation of neutrophil extracellular traps. *Cell Death Differ.* **26**, 395–408 (2019).

794 45. W. Wang, *et al.*, Identification of a novel chemokine (CCL28), which binds CCR10 (GPR2).
795 *J. Biol. Chem.* **275**, 22313–22323 (2000).

796 46. Y. Kobayashi, The role of chemokines in neutrophil biology. *Front. Biosci.* **13**, 2400–2407
797 (2008).

798 47. S. K. Ahuja, P. M. Murphy, The CXC Chemokines Growth-regulated Oncogene (GRO) α,
799 GROβ, GROγ, Neutrophil-activating Peptide-2, and Epithelial Cell-derived Neutrophil-
800 activating Peptide-78 Are Potent Agonists for the Type B, but Not the Type A, Human
801 Interleukin-8 Receptor. *Journal of Biological Chemistry* **271**, 20545–20550 (1996).

802 48. V. Marcos, *et al.*, CXCR2 mediates NADPH oxidase–independent neutrophil extracellular
803 trap formation in cystic fibrosis airway inflammation. *Nat. Med.* **16**, 1018–1023 (2010).

804 49. J. M. Rudd, *et al.*, Neutrophils Induce a Novel Chemokine Receptors Repertoire During
805 Influenza Pneumonia. *Front. Cell. Infect. Microbiol.* **9**, 108 (2019).

806 50. A. Craig, J. Mai, S. Cai, S. Jeyaseelan, Neutrophil recruitment to the lungs during bacterial
807 pneumonia. *Infect. Immun.* **77**, 568–575 (2009).

808 51. M. G. García-Patiño, R. García-Contreras, P. Licona-Limón, The Immune Response
809 against Acinetobacter baumannii, an Emerging Pathogen in Nosocomial Infections.
810 *Frontiers in Immunology* **8** (2017).

811 52. L. M. Grguric-Smith, *et al.*, Neutropenia exacerbates infection by Acinetobacter baumannii
812 clinical isolates in a murine wound model. *Frontiers in Microbiology* **6** (2015).

813 53. K. Yamada, *et al.*, Azithromycin attenuates lung inflammation in a mouse model of
814 ventilator-associated pneumonia by multidrug-resistant Acinetobacter baumannii.
815 *Antimicrob. Agents Chemother.* **57**, 3883–3888 (2013).

816 54. X. Zeng, *et al.*, Transcriptome Profiling of Lung Innate Immune Responses Potentially
817 Associated With the Pathogenesis of Acinetobacter baumannii Acute Lethal Pneumonia.
818 *Front. Immunol.* **11**, 708 (2020).

819 55. X. Zeng, *et al.*, A lethal pneumonia model of Acinetobacter baumannii: an investigation in
820 immunocompetent mice. *Clin. Microbiol. Infect.* **25**, 516.e1-516.e4 (2019).

821 56. H. H. Lee, *et al.*, Depletion of Alveolar Macrophages Increases Pulmonary Neutrophil
822 Infiltration, Tissue Damage, and Sepsis in a Murine Model of Acinetobacter baumannii
823 Pneumonia. *Infect. Immun.* **88** (2020).

824 57. R. R. Marchelletta, *et al.*, Salmonella-induced Diarrhea Occurs in the Absence of IL-8
825 Receptor (CXCR2)-Dependent Neutrophilic Inflammation. *J. Infect. Dis.* **212**, 128–136
826 (2015).

827 58. G. Nouailles, *et al.*, CXCL5-secreting pulmonary epithelial cells drive destructive
828 neutrophilic inflammation in tuberculosis. *J. Clin. Invest.* **124**, 1268–1282 (2014).

829 59. I. Stojiljkovic, A. J. Bäumler, F. Heffron, Ethanolamine utilization in Salmonella typhimurium:
830 nucleotide sequence, protein expression, and mutational analysis of the cchA cchB eutE
831 eutJ eutG eutH gene cluster. *J. Bacteriol.* **177**, 1357–1366 (1995).

832 60. M. Raffatellu, *et al.*, Lipocalin-2 resistance confers an advantage to Salmonella enterica
833 serotype Typhimurium for growth and survival in the inflamed intestine. *Cell Host Microbe*
834 **5**, 476–486 (2009).

835 61. R. Shamri, *et al.*, CCL11 elicits secretion of RNases from mouse eosinophils and their cell-
836 free granules. *FASEB J.* **26**, 2084–2093 (2012).

837 62. D.-Y. Cao, *et al.*, An ACE inhibitor reduces bactericidal activity of human neutrophils in vitro
838 and impairs mouse neutrophil activity in vivo. *Sci. Transl. Med.* **13** (2021).

839 63. L. Du, Y. Miao, X. Li, P. Shi, Z. Hu, A Novel and Convenient Method for the Preparation
840 and Activation of PRP without Any Additives: Temperature Controlled PRP. *Biomed Res.*
841 *Int.* **2018**, 1761865 (2018).

842 64. A. Carestia, *et al.*, Mediators and molecular pathways involved in the regulation of
843 neutrophil extracellular trap formation mediated by activated platelets. *J. Leukoc. Biol.* **99**,
844 153–162 (2016).

845 65. S. Liu, *et al.*, Neutrophil extracellular traps are indirectly triggered by lipopolysaccharide and
846 contribute to acute lung injury. *Sci. Rep.* **6**, 37252 (2016).

847 66. S. Masuda, *et al.*, Measurement of NET formation in vitro and in vivo by flow cytometry.
848 *Cytometry A* **91**, 822–829 (2017).

849 67. A. R. Moschen, *et al.*, Lipocalin 2 Protects from Inflammation and Tumorigenesis
850 Associated with Gut Microbiota Alterations. *Cell Host Microbe* **19**, 455–469 (2016).

851 68. A. J. J. Lammers, A. P. N. A. de Porto, O. J. de Boer, S. Florquin, T. van der Poll, The role
852 of TLR2 in the host response to pneumococcal pneumonia in absence of the spleen. *BMC*
853 *Infect. Dis.* **12**, 139 (2012).

854 69. P. Bankhead, *et al.*, QuPath: Open source software for digital pathology image analysis.
855 *Sci. Rep.* **7**, 16878 (2017).

856

857 **FIGURES AND LEGENDS**

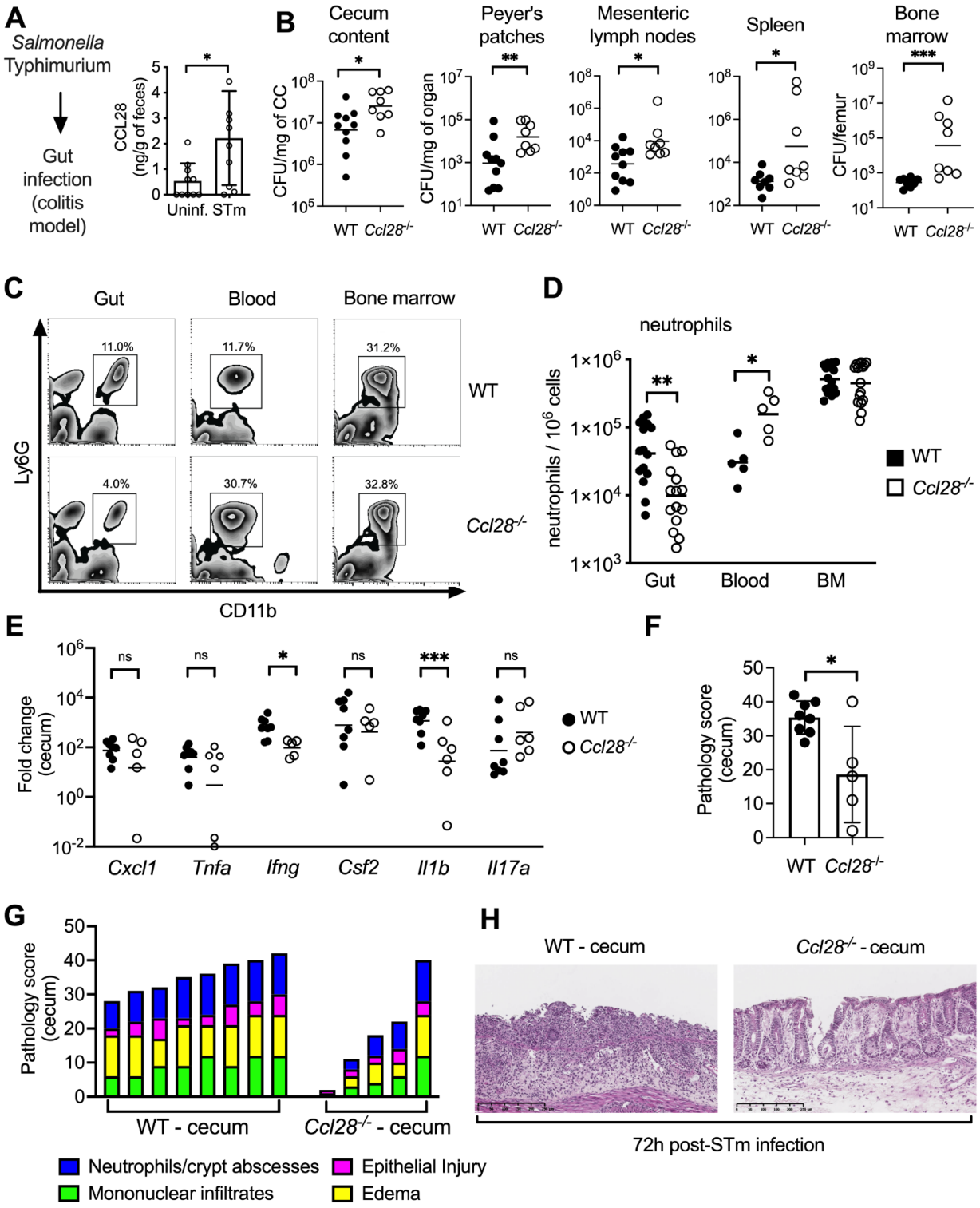

Figure 1

858

859 **Figure 1. CCL28 confers protection during *Salmonella* colitis and promotes neutrophil**
860 **accumulation in the gut**. (**A**) For the colitis model, wild-type mice were gavaged with
861 streptomycin 24h prior to oral infection with *S. enterica* serovar Typhimurium (STm). At 96h post-
862 infection, CCL28 in feces was quantified by ELISA. Data shown comprise two independent
863 experiments (uninfected, n=10; STm, n=10). Bars represent the mean ± SD. (**B**) CFU in cecum
864 content, Peyer's patches, mesenteric lymph nodes, spleen, and bone marrow were determined
865 at 72h post-infection of wild-type (WT, black circles) and *Ccl28*$^{-/-}$ (white circles) littermate mice.
866 Data shown comprise three independent experiments (WT, n=10; *Ccl28*$^{-/-}$, n=8). Some of the
867 spleen data points were published as a preliminary characterization in Burkhardt et al. (Ref 9) and
868 are combined with the new dataset. Bars represent the geometric mean. (**C**) Representative
869 contour plots of neutrophils (CD11b^{+} Ly6G^{+} cells; gated on live, CD45^{+} cells) obtained from the
870 gut, blood, and bone marrow of STm-infected WT or *Ccl28*$^{-/-}$ mice, as determined by flow
871 cytometry at 48h post-infection. (**D**) Frequency of neutrophils per million live CD45+ cells obtained
872 from the gut, blood, and bone marrow of STm-infected WT (black bars) or *Ccl28*$^{-/-}$ mice (white
873 bars). Data shown comprise three independent experiments (WT, n=15; *Ccl28*$^{-/-}$, n=15; blood was
874 collected from n = 5 per group). Bars represent the mean ± SD. (**E**) Relative expression levels
875 (qPCR) of *Cxcl1* (CXCL1), *Tnfa* (TNFα), *Ifng* (IFNγ), *Csf2* (GM-CSF), *Il1b* (IL-1β), and *Il17a* (IL-
876 17A) in the cecum of WT (black circles, n=8) or *Ccl28*$^{-/-}$ mice (white circles, n=6). Bars represent
877 the geometric mean. Data shown comprise three independent experiments. (**F-H**)
878 Histopathological analysis of cecum collected from STm-infected WT or *Ccl28*$^{-/-}$ mice (WT, n=8;
879 *Ccl28*$^{-/-}$, n=5). (**F**) Sum of the total histopathology score, (**G**) histopathology scores showing the
880 analyzed parameters, and (**H**) H&E-stained sections from one representative animal for each
881 group (200X). (**F**) Bars represent the mean ± SD. Mann-Whitney U was used for all datasets
882 where statistical analysis was performed. A significant change relative to WT controls is indicated
883 by $^{*}p \leq 0.05$, $^{**}p \leq 0.01$, $^{***}p \leq 0.001$. ns = not significant.

884

885

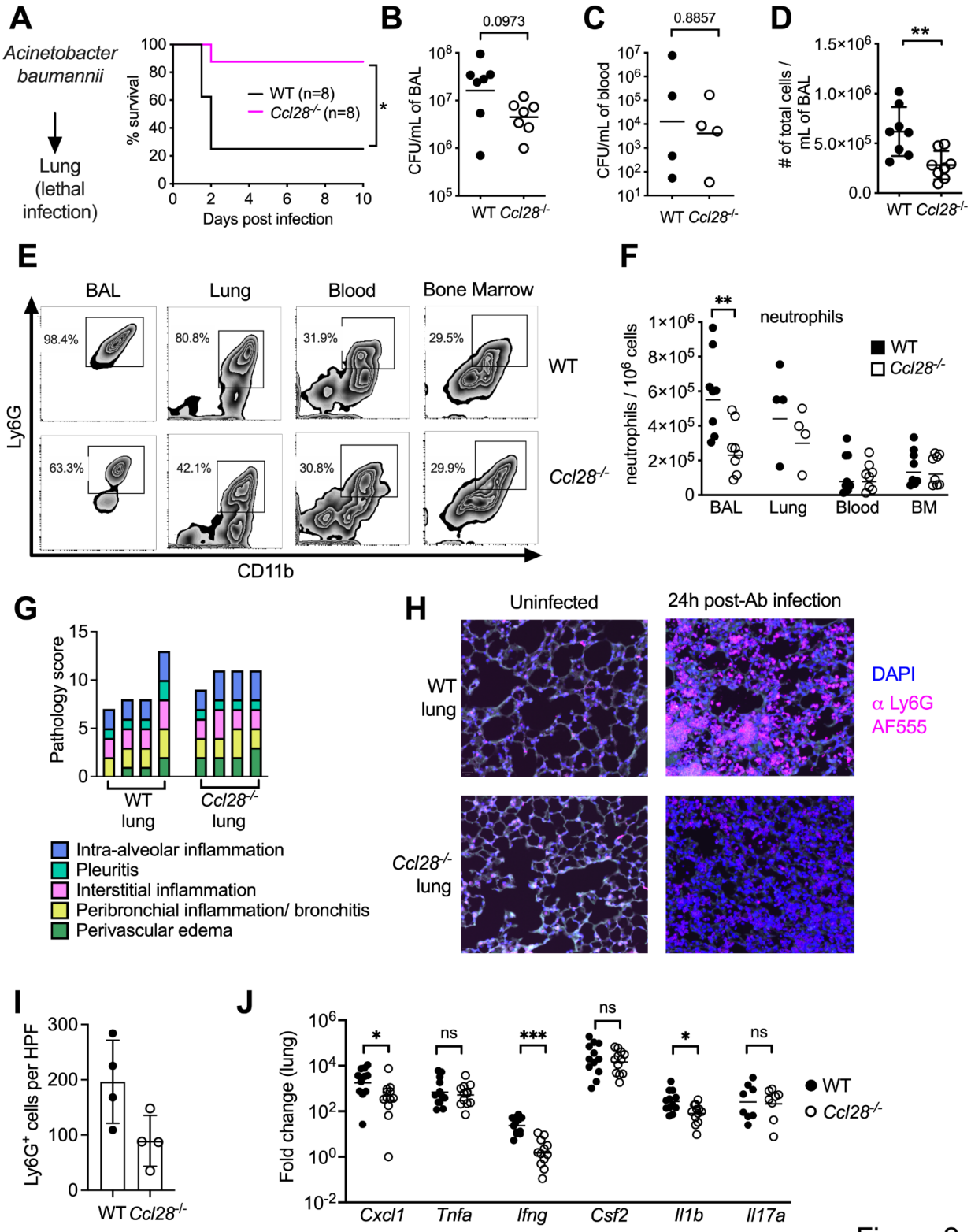

Figure 2

886

887

888 **Figure 2. Absence of CCL28 confers protection in a lethal *Acinetobacter* pneumonia model.**
889 (**A**) WT mice (black line) and *Ccl28*$^{-/-}$ mice (magenta line) were intratracheally infected with
890 *Acinetobacter baumannii* (Ab) and their survival was determined for 10 days. Data shown
891 comprise two independent experiments (WT, n=8; *Ccl28*$^{-/-}$, n=8). (**B-F**) WT and *Ccl28*$^{-/-}$ mice were
892 compared 24h post-infection with Ab. (**B, C**) Ab CFU in (**B**) BAL (bronchoalveolar lavage) fluid or
893 (**C**) blood in WT mice (black circles) and *Ccl28*$^{-/-}$ mice (white circles). (**D**) The number of total host
894 cells per mL of BAL, as determined by flow cytometry. (WT, n=8; *Ccl28*$^{-/-}$, n=8) (**E, F**)
895 Representative (**E**) contour plots of neutrophils (CD11b^{+} Ly6G^{+} cells; gated on live, CD45^{+} cells)
896 and (**F**) frequency of neutrophils obtained from the BAL, lung, blood, and bone marrow of Ab-
897 infected WT or *Ccl28*$^{-/-}$ mice, as determined by flow cytometry. Data comprise two independent
898 experiments (WT, n=8; *Ccl28*$^{-/-}$, n=8; lung was collected from n = 4 per group). Bars represent (**B,**
899 **C**) the geometric mean or (**D, F**) the mean ± SD. (**G**) Histopathological analysis of lungs from WT
900 and *Ccl28*$^{-/-}$ mice infected with Ab at 24 h post-infection. Each bar represents an individual mouse.
901 (**H**) Representative immunofluorescence image of lungs from WT and *Ccl28*$^{-/-}$ mice, uninfected or
902 infected with Ab stained for the neutrophil marker Ly6G (magenta). DAPI (blue) was used to label
903 nuclei. (**I**) Quantification of Ly6G^{+} cells per high-power field (HPF) from immunofluorescence
904 images of lungs from WT mice (n=4) and *Ccl28*$^{-/-}$ mice (n=4). Bars represent the mean ± SD. (**J**)
905 Relative expression levels (qPCR) of *Cxcl1* (CXCL1), *Tnfa* (TNFα), *Ifng* (IFNγ), *Csf2* (GM-CSF),
906 *Il1b* (IL-1β), and *Il17a* (IL-17A) in the lung of WT (black circles, n=12) or *Ccl28*$^{-/-}$ mice (white circles,
907 n=12) infected with Ab. Bars represent the geometric mean. Data shown comprise three
908 independent experiments. Mann-Whitney U was used for all datasets where statistical analysis
909 was performed. A significant change relative to WT controls is indicated by *$p \leq 0.05$, **$p \leq 0.01$,
910 ***$p \leq 0.001$. ns = not significant.
911
912

913

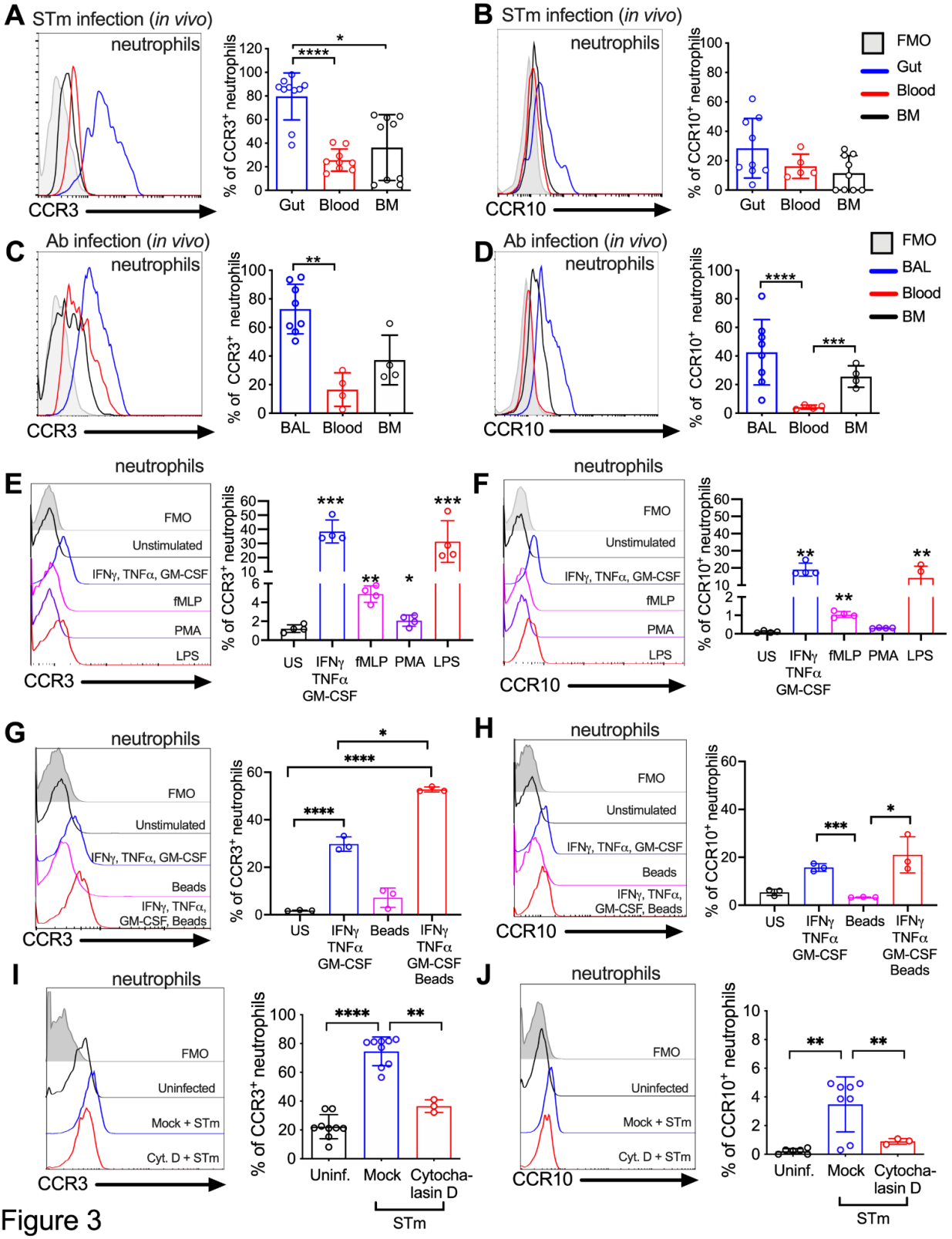

Figure 3

914

915

916 **Figure 3. Surface expression of the CCL28 receptors CCR3 and CCR10 on neutrophils from**
917 **infected tissue, and upon stimulation with proinflammatory stimuli and phagocytosis. (A-**
918 **D)** Surface expression of (**A, C**) CCR3 or (**B, D**) CCR10 on neutrophils obtained from (**A, B**) the
919 gut, blood, and bone marrow (BM) 72h post-infection with STm, or (**C, D**) the BAL, blood, and
920 bone marrow 24h post-infection with Ab, analyzed by flow cytometry. Left panels show
921 representative histograms of (**A, C**) CCR3 or (**B, D**) CCR10 expression on the surface of
922 neutrophils (gated on live, $CD45^+$ $CD11b^+$ $Ly6G^+$ cells) from (**A, B**) the gut (blue), blood (red), and
923 bone marrow (BM; black) or (**C, D**) BAL (blue), blood (red), and bone marrow (BM; black). Right
924 panels show the percentage of (**A, C**) $CCR3^+$ or (**B, D**) $CCR10^+$ neutrophils obtained from (**A, B**)
925 gut, blood, and BM or (**C, D**) BAL, blood, and BM. Data are from two independent experiments.
926 (**E-H**) Uninfected bone marrow neutrophils were unstimulated or treated with the indicated stimuli
927 for 4h. Surface expression of (**E**, **G**) CCR3 and (**F**, **H**) CCR10 on neutrophils was determined by
928 flow cytometry. Left panels show representative histograms of (**E**, **G**) CCR3 or (**F**, **H**) CCR10
929 surface expression after stimulation with: (**E, F**) cytokines IFNγ + TNFα + GM-CSF (blue); fMLP
930 (magenta); PMA, (purple); LPS (red); (**G, H**) cytokines IFNγ + TNFα + GM-CSF (blue); beads
931 alone (magenta); cytokines plus beads (red). Right panels show the percentage of (**E, G**) $CCR3^+$
932 or (**F**, **H**) $CCR10^+$ neutrophils following stimulation with the indicated stimuli. US = unstimulated.
933 Data shown are representative of two independent experiments. (**I, J**) Bone marrow neutrophils
934 were infected with opsonized STm at a multiplicity of infection (MOI)=10 for 1h with (red) or without
935 (blue) pretreatment with cytochalasin D for 30 min before infection. Surface expression of (**I**)
936 CCR3 or (**J**) CCR10 was determined by flow cytometry. Data are from three independent
937 experiments. Left panels show representative histograms of surface receptor staining on
938 neutrophils, and right panels show the percentages. (**A-J**, right panels) Bars represent the mean
939 ± SD. (**A-D, I, J**) Log-transformed data were analyzed by one-way ANOVA for independent
940 samples, assuming non-equal SD given the differences in the variance among the groups and

941 followed by Dunnett's multiple comparisons test. (**E-H**) Data were analyzed by one-way ANOVA
942 for paired samples, applying the Greenhouse-Geisser correction given the differences in variance
943 among the groups; (**E, F**) Dunnett's multiple comparison test was performed to compare the
944 different conditions of stimulation with the control group; (**G, H**) Tukey's multiple comparison test
945 was performed to compare each condition to each other. Significant changes are indicated by *p
946 ≤ 0.05, **$p \leq 0.01$, ***$p \leq 0.001$, ****$p \leq 0.0001$.

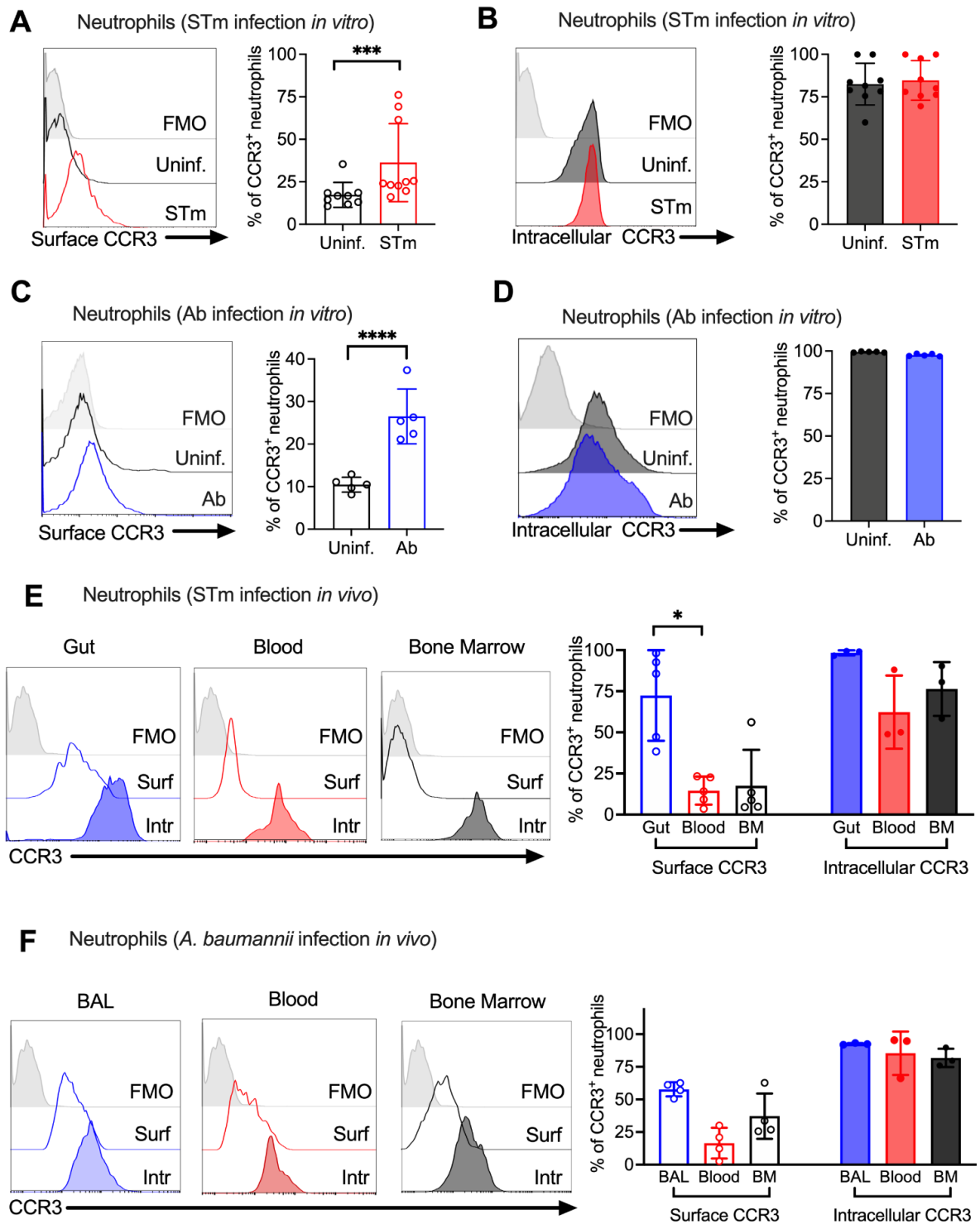

Figure 4

947

948

949

950 **Figure 4. Neutrophil CCR3 is stored in intracellular compartments and rapidly mobilizes to**
951 **the cell surface during infection.** (**A-D**) Bone marrow neutrophils were infected at MOI=10 with
952 (**A, B**) opsonized *Salmonella enterica* serovar Typhimurium (STm) for 1h or (**C, D**) *Acinetobacter*
953 *baumannii* (Ab) for 4h. (**A, C**) Surface CCR3 or (**B, D**) intracellular CCR3 were detected by flow
954 cytometry. (**E, F**) Neutrophils were obtained from (**E**) the gut, blood, and bone marrow 72h post-
955 infection with STm or (**F**) BAL, blood, and bone marrow 24h post-infection with Ab. Surface (clear
956 histograms) or intracellular (solid histograms) CCR3 expression was analyzed by flow cytometry.
957 (**A-F**) Left panels show representative histograms, and right panels show the percentage of
958 neutrophils expressing CCR3 on their surface (clear bars) or intracellularly (solid bars). Bars
959 represent the mean ± SD. Data was analyzed by paired *t* test (A-D) or one-way ANOVA followed
960 by Dunnett's multiple comparison test (E and F) on log-transformed data. Significant changes are
961 indicated by $^{*}p \leq 0.05$, $^{***}p \leq 0.001$, $^{****}p \leq 0.0001$

962

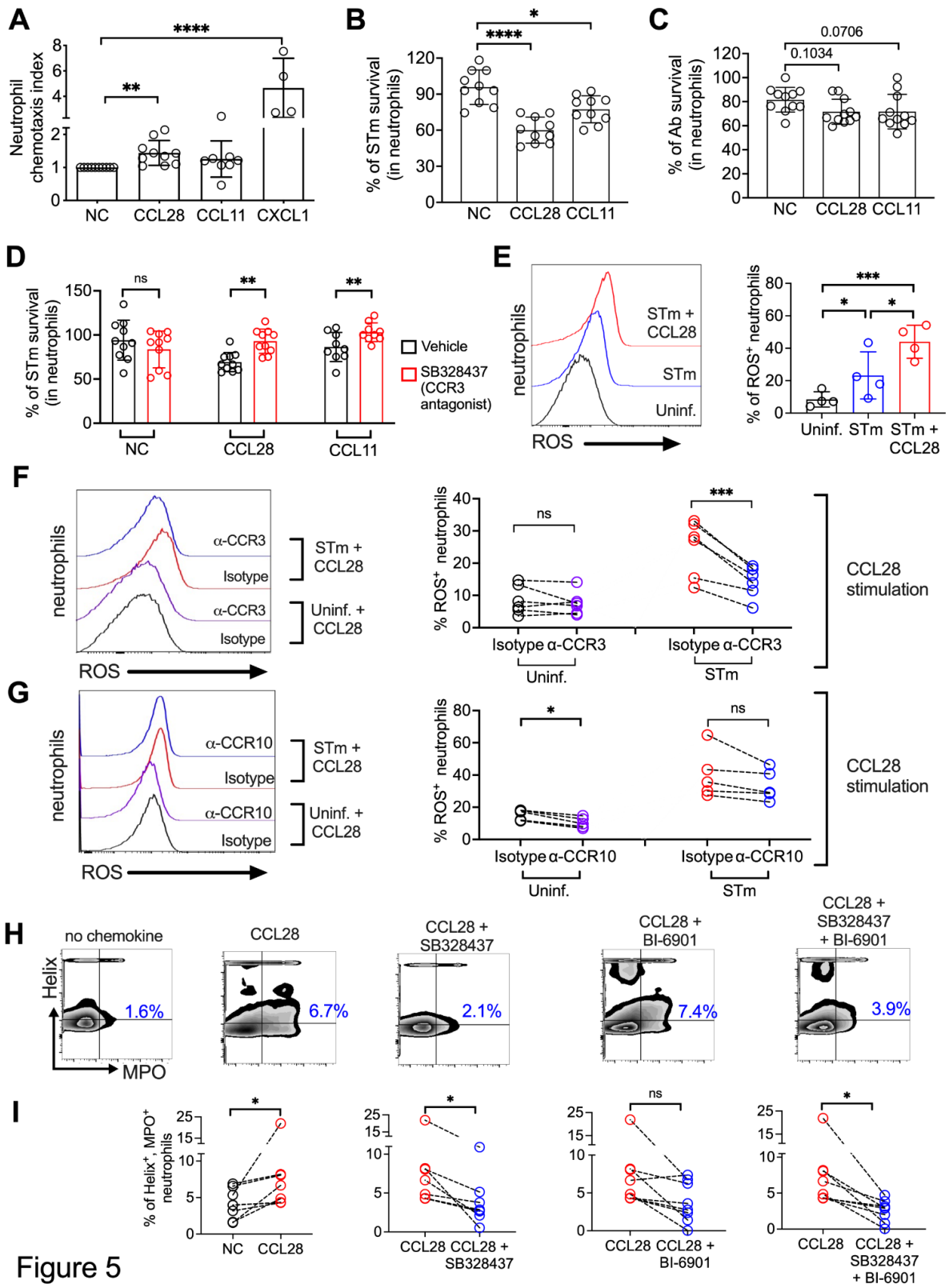
A
Neutrophil chemotaxis index
NC
CCL28
CCL11
CXCL1
B
% of STm survival (in neutrophils)
C
% of Ab survival (in neutrophils)
0.0706
0.1034
D
% of STm survival (in neutrophils)
ns
Vehicle
SB328437 (CCR3 antagonist)
E
neutrophils
STm + CCL28
STm
Uninf.
ROS
% of ROS+ neutrophils
F
α-CCR3
Isotype
STm + CCL28
Uninf. + CCL28
% ROS+ neutrophils
Isotype α-CCR3
CCL28 stimulation
G
α-CCR10
Isotype α-CCR10
H
no chemokine
CCL28
CCL28 + SB328437
CCL28 + BI-6901
CCL28 + SB328437 + BI-6901
Helix
MPO
1.6%
6.7%
2.1%
7.4%
3.9%
I
% of Helix+, MPO+ neutrophils

Figure 5

965 **Figure 5. CCL28 enhances neutrophil antimicrobial activity**. (**A**) Murine bone marrow
966 neutrophils were stimulated with IFNγ + TNFα + GM-CSF for 4h before adding $1x10^6$ cells to the
967 upper compartment of a transwell chamber for chemotaxis assays. Each of the chemokines
968 (CCL28, CCL11, or CXCL1), or no chemokine (NC), were placed in separate lower
969 compartments. The transwell plate was incubated for 2h at 37°C. Cells that migrated to the lower
970 compartment were enumerated by flow cytometry. Neutrophil chemotaxis index was calculated
971 by taking the number of cells that migrated in response to a chemokine and dividing it by the
972 number of cells that migrated in the absence of a chemokine. Data are from four independent
973 experiments. (**B, C**) Infection of bone marrow neutrophils. (**B**) Opsonized STm ($1x10^7$ CFU) or
974 (**C**) opsonized Ab ($1x10^7$ CFU) were cultured alone, or added to bone marrow neutrophils ($1x10^6$
975 cells) stimulated with CCL28, CCL11, or no chemokine, for 2.5h (STm) or 4.5h (Ab) at 37°C. CFU
976 were enumerated by plating serial dilutions. Percentage of bacterial survival was calculated for
977 each condition by taking the CFU from bacteria incubated with neutrophils and dividing it by the
978 CFU from bacteria incubated without neutrophils, multiplied by 100. Data shown for each infection
979 comprise three independent experiments. Bars represent the mean ± SD. (**D**) The effect of the
980 CCR3 antagonist SB328437 on neutrophil-mediated STm killing was evaluated by performing the
981 experiment as described in panel (**B**), with or without the antagonist. Data shown comprise three
982 independent experiments. (**E-G**) ROS production (H_2DCFDA conversion to fluorescent DCF)
983 detected by flow cytometry in bone marrow neutrophils infected with STm as described in panel
984 (**B**). In (**F, G**), cells were stimulated with CCL28 in the presence of an anti-CCR3 antibody, an
985 anti-CCR10 antibody, or isotype controls. Left panels show representative histograms, and right
986 panels show the percentage of ROS^+ neutrophils in the indicated treatment groups. (**H, I**) NET
987 formation ($Helix^+$ MPO^+ neutrophils) detected by flow cytometry in human neutrophils activated
988 with platelets. As indicated, cells were unstimulated (NC), stimulated with CCL28 alone, or with
989 CCL28 and the CCR3 antagonist SB328437 and/or the CCR10 antagonist BI-6901. (**H**)
990 Representative contour plots, and (**I**) percentage of $Helix^+$ MPO^+ neutrophils in the indicated

treatment groups. (**A**-**E**) Bars represent the mean ± SD. (**A**) Log-transformed data were analyzed by non-parametric ANOVA (Kruskal-Wallis's test), assuming non-equal SD given the differences in the variance among the groups, followed by Dunn's multiple comparisons test. (**B, C**) Log-transformed data were analyzed by one-way ANOVA for paired samples, applying the Greenhouse-Geisser correction given the differences in the variance among the groups. Dunnett's multiple comparison test was performed to compare the treatment groups only with the control group. (**D, I**) Log-transformed data were analyzed by paired *t* test. (**E-G**) Log-transformed data were analyzed by one-way ANOVA for paired samples. Greenhouse-Geisser correction was applied in **F** and **G** given the differences in variance among the groups. Tukey's multiple comparison test was performed to compare all conditions to each other. Significant changes are indicated by *$p \leq 0.05$, **$p \leq 0.01$, ***$p \leq 0.001$ ****$p \leq 0.0001$. ns = not significant.

1015 **SUPPLEMENTAL FIGURES**

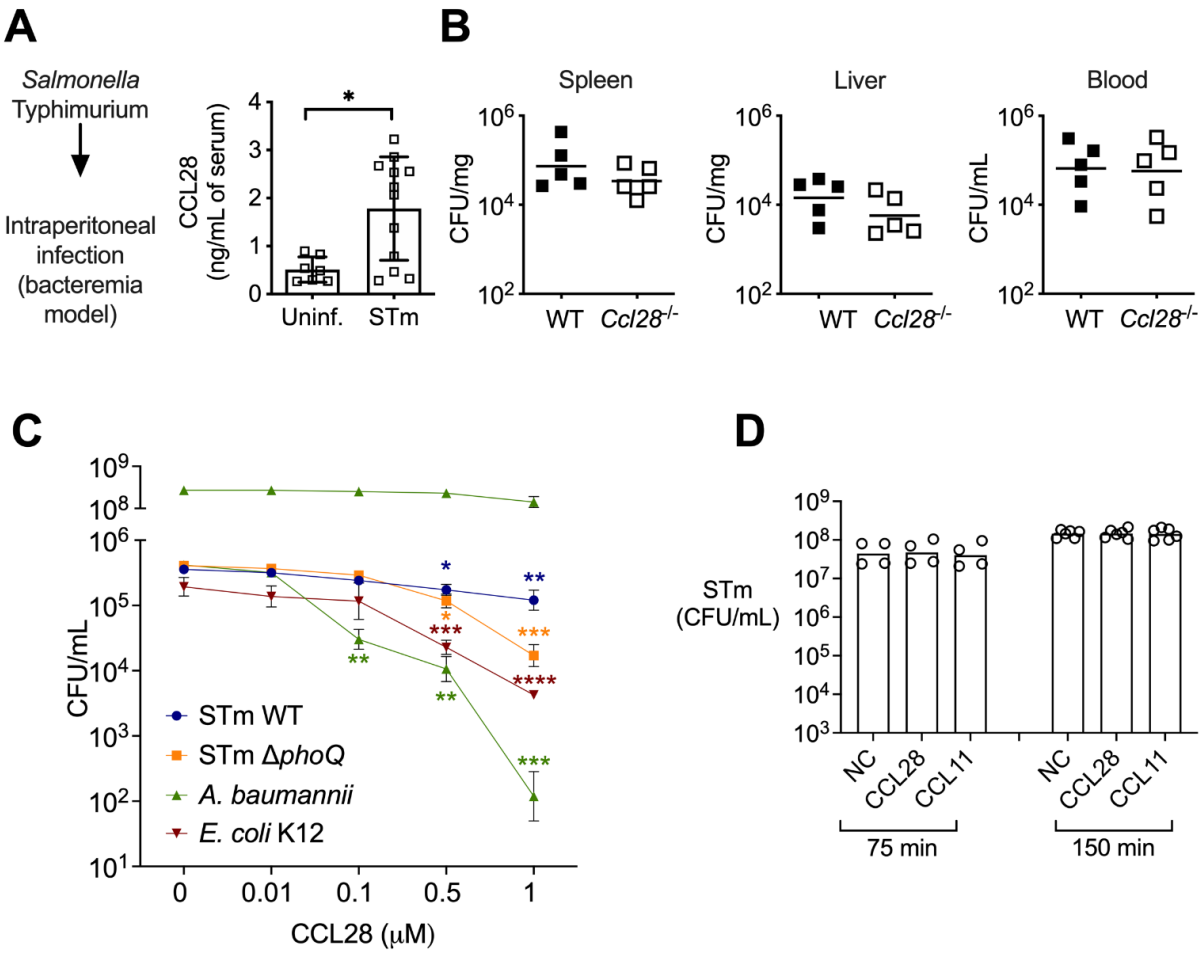

1016 Supp. Fig. 1

1017

1018 **Supplementary Figure 1. CCL28 does not confer protection in a *Salmonella***
1019 **bacteremia model, and lacks direct antimicrobial activity against *Salmonella*.**
1020 (**A, B**) For the bacteremia model, mice were infected by intraperitoneal injection with *S.*
1021 Typhimurium (STm, $1x10^3$ CFU) or sterile PBS (uninfected control). (**A**) At 96h post-infection,
1022 CCL28 in serum was quantified by ELISA of wild-type mice (uninfected, n=7; STm, n=12). Data
1023 shown comprise two independent experiments. Bars represent the mean ± SD. (**B**) STm CFU
1024 was determined in the spleen, liver, and blood of WT mice (black squares) and *Ccl28*$^{-/-}$ mice (white
1025 squares) 96h after intraperitoneal infection with STm ($1x10^3$ CFU). Data shown comprise two
1026 independent experiments (WT, n=5; *Ccl28*$^{-/-}$, n=5). (**C, D**) *In vitro* antimicrobial activity of CCL28
1027 against STm wild-type, STm *ΔphoQ*, *E. coli* K12, and *A. baumannii*. (**C**) $5x10^5$ CFU/mL of each
1028 strain (*A. baumannii* additionally at $5x10^8$ CFU/mL) was incubated with recombinant murine
1029 CCL28 at the indicated concentrations (n=4 per group), and CFU were enumerated after 2h. (**D**)
1030 STm wild-type ($1x10^7$ CFU/mL) was incubated with recombinant murine CCL28 (50 nM) or CCL11
1031 (25 nM) and CFU were enumerated at 75 min (n=4 per group) and 150 min (n=6 per group). Bars
1032 represent the geometric mean. (**A**) Data were analyzed by Mann-Whitney U relative to uninfected
1033 controls. (**C**) Log-transformed data were analyzed by nonparametric one-way ANOVA (Kruskal-
1034 Wallis) for independent samples. Dunn's multiple comparison test was performed to compare
1035 bacterial CFU at each time point relative to time zero (control group). Significant changes are
1036 indicated by $*p \leq 0.05$, $**p \leq 0.01$, $***p \leq 0.001$ $****p \leq 0.0001$.

1037

1038

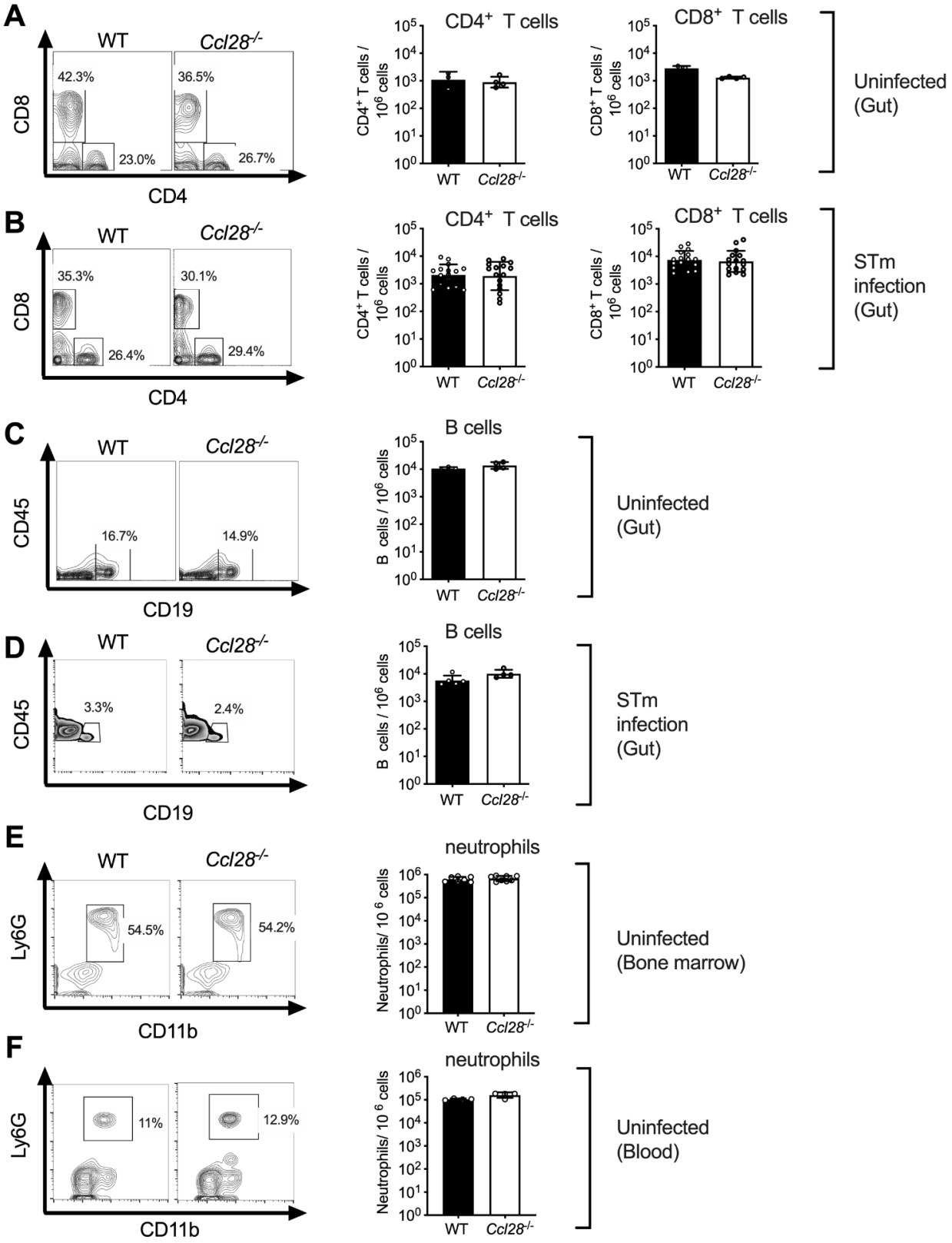

Supp. Fig. 2

1039

1040 **Supplementary Figure 2**. **Wild-type and *Ccl28*$^{-/-}$ mice exhibit similar numbers of T and B**
1041 **cells, as well as bone marrow and blood neutrophils.**
1042 Flow cytometry analysis of (**A**, **B**) CD4^{+} and CD8^{+} T cells, and (**C**, **D**) CD19^{+} B cells isolated from
1043 the gut of (**A, C**) uninfected WT and *Ccl28*$^{-/-}$ mice or (**B, D**) WT and *Ccl28*$^{-/-}$ mice infected with STm
1044 for 48h (colitis model; see also **Fig. 1**). (**E, F**) Cells from (**E**) bone marrow or (**F**) blood of uninfected
1045 WT (black bars) or *Ccl28*$^{-/-}$ (white bars) mice were analyzed by flow cytometry to determine the
1046 percentage and number of neutrophils. (**A-F**) Left panels show representative contour plots. Right
1047 panels show the frequency of the indicated cells per million CD45+ live cells of WT mice (black
1048 bars) and *Ccl28*$^{-/-}$ mice (white bars). Each circle represents a mouse. Bars represent the geomean
1049 ± SD.
1050
1051
1052

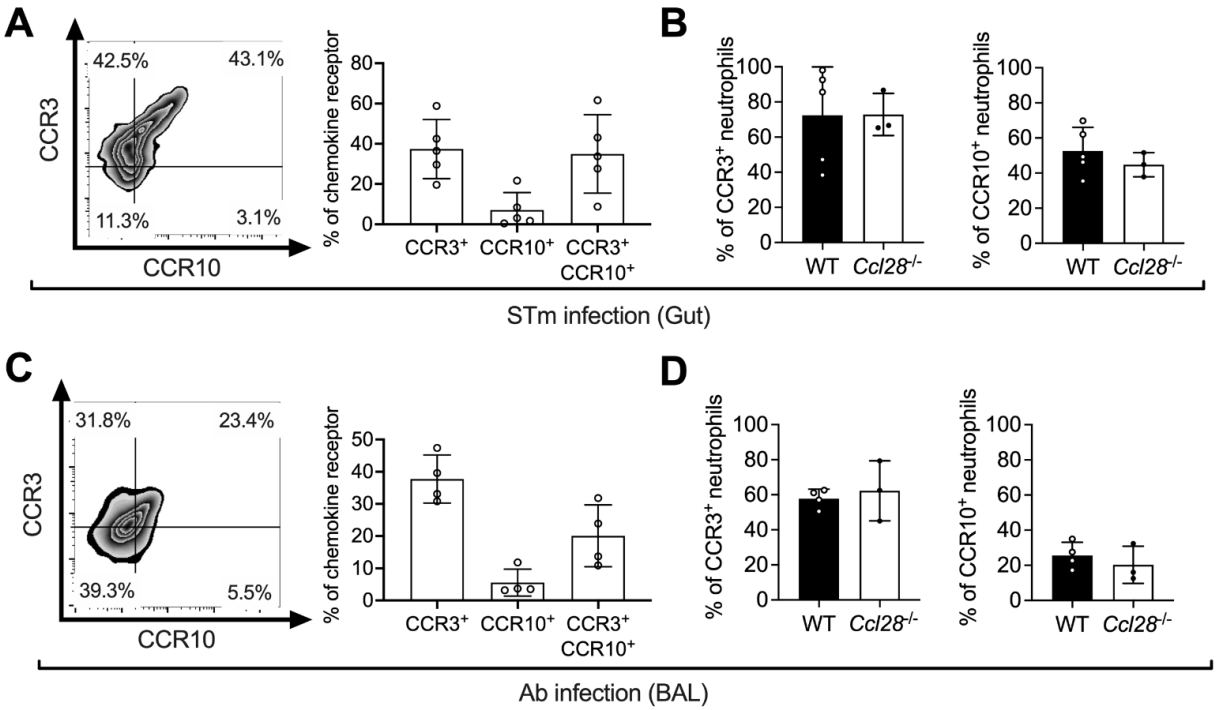
A
42.5%
43.1%
11.3%
3.1%
CCR3
CCR10
% of chemokine receptor
CCR3+
CCR10+
CCR3+ CCR10+
B
% of CCR3+ neutrophils
% of CCR10+ neutrophils
WT
Ccl28-/-
STm infection (Gut)
C
31.8%
23.4%
39.3%
5.5%
D
Ab infection (BAL)

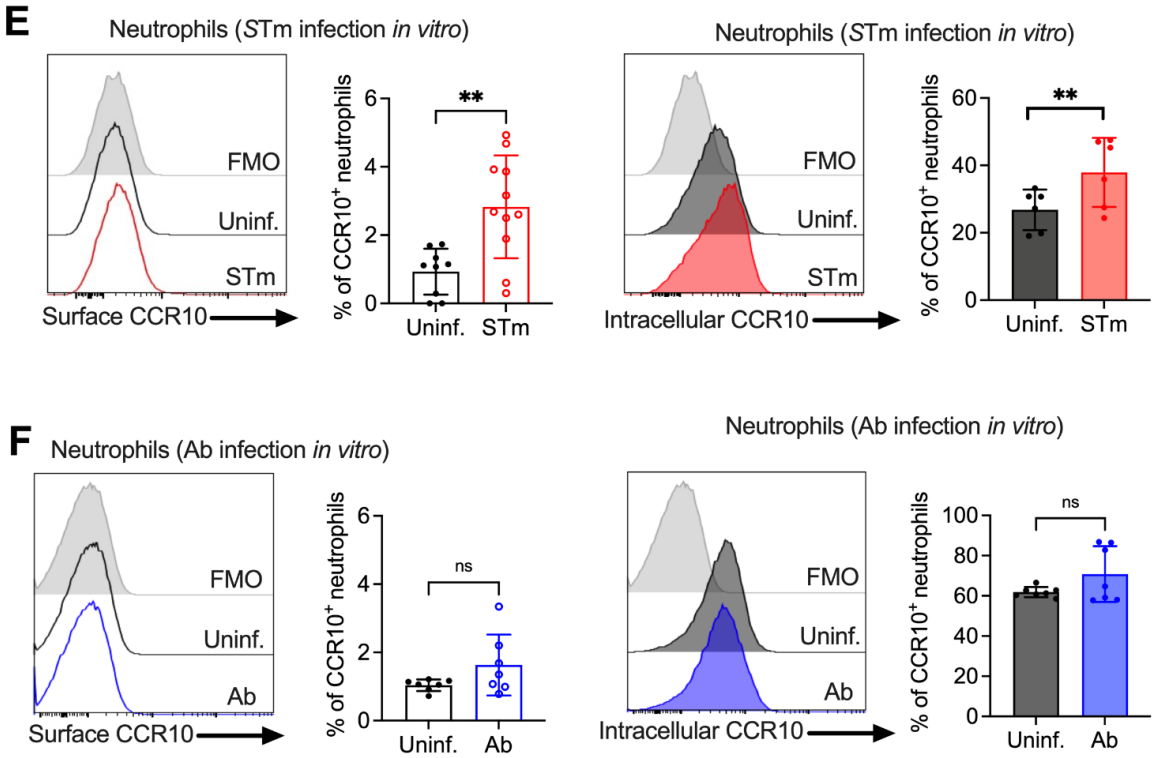
E
Neutrophils (STm infection in vitro)
FMO
Uninf.
STm
Surface CCR10
Intracellular CCR10
% of CCR10+ neutrophils
**
Uninf.
STm
F
Neutrophils (Ab infection in vitro)
Ab
ns

Supp. Fig. 3

1055 **Supplementary Figure 3**. **Expression of CCR3 and CCR10 in neutrophils isolated from the**
1056 **gut and lung mucosa, and CCR10 in neutrophils infected *in vitro*.**
1057 (**A**) Surface expression of CCR3 and CCR10 on neutrophils obtained from the gut of WT mice
1058 (n=5) infected with STm for 72h, analyzed by flow cytometry. (**B**) Percentage of $CCR3^+$ and
1059 $CCR10^+$ neutrophils obtained from the gut of WT (n=5) and *Ccl28*$^{-/-}$ mice (n=3) infected with STm
1060 for 72h, analyzed by flow cytometry. (**C**) Surface expression of CCR3 and CCR10 on neutrophils
1061 obtained from the BAL of WT mice (n=4) infected with Ab for 24h, analyzed by flow cytometry.
1062 (**D**) Percentage of $CCR3^+$ and $CCR10^+$ neutrophils obtained from the BAL of WT (n=4) and *Ccl28*$^{-}$
1063 $^{/-}$ mice (n=3) infected with Ab for 24h, analyzed by flow cytometry. (**A**, **C**) Left panels show
1064 representative contour plots, and right panels show the percentages of neutrophils expressing
1065 the indicated receptor on their surface. Bars represent the mean ± SD. (**E, F**) Bone marrow
1066 neutrophils were infected with (**E**) opsonized STm at MOI=10 for 1h or (**F**) Ab at MOI=10 for 4h.
1067 Surface (clear histograms) or intracellular (solid histograms) CCR10-expressing neutrophils were
1068 detected by flow cytometry. Left panels show representative histograms, and right panels show
1069 the percentage of neutrophils expressing CCR10 on their surface (clear bars) or intracellularly
1070 (solid bars). (**E, F**) A significant change (paired *t* test) relative to uninfected controls is indicated
1071 by $^{**}p \leq 0.01$; ns = not significant.
1072
1073